IN-51-CR

304618

FINAL REPORT OF NAG 2-615

COSMOS 2044

SEPTEMBER 14, 1990

Oliver H. Lowry, Igor Krasnov, E. Ilyina Kakueva, Patti M. Nemeth,
David B. McDougal, Jr., Rati Choksi, Joyce G. Carter, Maggie M. Y. Chi,
Jill K. Manchester and Mary Ellen Pusateri

PART I. Metabolic Enzymes of Individual Muscle Fibers

Individual fibers of any given muscle vary widely in enzyme composition, a fact obscured when enzyme levels of whole muscle are measured. Therefore, the purpose of this part of the study was to assess the effects of microgravity and hind limb suspension on the enzyme patterns within a slow twitch muscle (soleus) and a fast twitch muscle (tibialis anterior).

The samples for assay were prepared in two different ways. In the first case, a 3-5 mg piece of each muscle was freeze-dried at -35°C. Portions of individual fibers, 2-3 mm long, were dissected free, weighed, the length measured, and then stored separately under vacuum at -70°C. Most of the enzymes from a given fiber were measured in a single extract prepared from a dry sample weighing about 0.5 μg (0.5 to 1 mm long). This was added to 5 μl of special detergent-containing medium known to preserve without loss all but a few of the enzymes of interest during storage at -70°C. After initial incubation for 2 hours at room temperature (to permit extraction and even distribution of the enzymes), the samples were transferred to a -70°C freezer. Since each assay required only 0.1 to 0.2 μl of extract (equivalent to 10 to 20 ng of dry fiber), the single 5 μl extract was sufficient for duplicate assays of a large number of enzymes.

In a few special cases, assays were performed on single 10 to 20 ng samples added directly to the appropriate specific reagent.

The alternate method used to prepare samples for assay was to cut frozen cross sections at -20°C from a piece of the original frozen muscle. Thinner sections (16 μm) were stained for myosin ATPase to type the individual fibers. Alternate thicker slices (32 μm) were freeze-dried at -35°C and samples were dissected from individual fibers identified as to type by the adjacent stained sections.

(NASA-CR-187003) COSMOS 2044 Final Report (Washington Univ.) 51 p CSCL 06C

N91-14702

Unclas
G3/51 0304618

These studies were made on 95 soleus fibers and about 300 tibialis anterior (TA) fibers. Each of the soleus fibers was analyzed for 4 or 5 different enzymes, and 139 TA fibers were assayed for 3 to 5 different enzymes. Other single TA fibers were assayed for an additional 3 enzymes. Altogether, over 2200 individual enzyme measurements were made.

The enzymes were selected for assay in view of the results obtained in the previous Cosmos flight (1887), and the known metabolic enzyme characteristics of fast and slow muscle fibers. For example, TA fibers were first assayed for malate dehydrogenase, hexokinase, and thiolase, all of which had increased markedly in the TA flight muscles; in addition, they are highly variable among TA fibers. Similarly, soleus fibers were initially assayed for hexokinase because it was markedly increased in the 1987 Cosmos flight fibers, and for pyruvate kinase because it was consistently variable among control soleus fibers, and had increased in the fibers of at least one soleus flight muscle of the earlier Cosmos experiment.

Fibers were obtained from synchronous rats 6 and 7 (S6, S7), flight rats 6 and 7 (F6, F7) and tail suspension rats 6 and 7 (T6, T7).

RESULTS

SOLEUS MUSCLE

Average values.

Table 1 gives average values for size and activities of five enzymes in 15 or 16 fibers from soleus muscles of rats S6 and S7, F6 and F7, and T6 and T7.

Size.

Average fiber size was much smaller for both flight and tail suspension muscles ($P < 0.01$) than for either S6 or S7. The average dry weight loss was 38% for T6 and T7 and 36% for F6 and F7.

The dry weights (μg per mm) are based on the assumption that all the muscles were frozen at the same fraction of their resting lengths, and are subject to error if this were not the case. With

this proviso it is interesting to compare these dry weight losses with the losses in wet weight of the whole and soleus muscles: 20% and 3% respectively for F6 and F7, and 27% and 29% respectively for T6 and T7. Even if F7 is ignored because the wet weight value is so far out of line, it seems clear that the fibers lost relatively more dry weight than the loss in total mass. Thus, there must have been an increase in relative H_2O content, either in the fibers themselves or the extracellular space or both.

Soleus enzymes that are usually higher in fast-twitch than slow twitch muscle.

Pyruvate kinase was higher in fibers of both flight muscles and both tail suspension muscles than in either synchronous muscle. The increases were respectively 43% and 38% in F6 and F7, and 126% and 7% in T6 and T7. Only the increases in F7 and T6 were statistically significant.

Glycerol-3-phosphate dehydrogenase (GOPDH) was on average also higher than either S6 or S7 in fibers of both flight and tail suspension muscles with $P \leq 0.05$ in each case. The increases were equal or greater than for pyruvate kinase: 65% and 46% respectively in F6 and F7, and 126% and 44% in T6 and T7.

P-fructokinase was higher in fibers of both F7 and T7 than in S7 (the only muscles analyzed for this enzyme). The differences, however, were small (+27% and +18% respectively), and not statistically significant in either case.

Two soleus enzymes usually higher in slow-twitch muscles.

Hexokinase was higher in the fibers of both flight and both tail suspension muscles than in S7 (the higher of the two synchronous muscles). The differences were statistically significant ($P < 0.02$ in all cases). Relative to the average for S6 and S7, the respective increases were 35% and 60% for F6 and F7, and 31% and 108% for T6 and T7.

3-ketoacid CoA transferase was the only one of the five enzymes which was decreased in the fibers of either flight or tail suspension muscles, and the differences were not great although

statistically significant ((P ≤ 0.05 in all but T7). The changes relative to the lower of the two synchronous muscle values were -10% for both F6 and F7, and respectively -21% and -2% for T6 and T7.

Individual soleus fiber values.

The above average values obscure the large differences among fibers in size and enzyme levels and the degree of correlation between different enzymes in individual fibers.

Figs. 1 to 3 compare GOPDH and pyruvate kinase activities in 15 or 16 fibers from each of the 6 muscles. In both S6 and S7 (Fig. 1) the two enzymes vary coordinately over a range of about 2.5-fold in each case. The correlation coefficients (r) are 0.801 for S6 and 0.77 for S7, both highly significant (P < 0.001). For F6 and F7 (Fig. 2), the activity ranges are both increased to about 5-fold for F6 and 3- to 4-fold for F7. The correlation coefficients are increased to 0.961 and 0.948 for fibers from the two respective muscles. Very similar effects are seen for T6 and T7 (Fig. 3) with values for half or more of the fibers rising above the control boundary zone for S6 and S7.

Correlations between phosphofructokinase and pyruvate kinase for S7, F7 and T7 were similar to those for GOPDH and pyruvate kinase. The r values were 0.705, 0.793, and 0.886 respectively, with P < 0.01 in each case (data not shown in a figure).

Hexokinase was also positively correlated with pyruvate kinase among fibers from S6 (r = 0.524, P < 0.05) and S7 (r = 0.819, P < 0.001) (Fig. 4). However, no significant positive or negative correlations were observed between these two enzymes among flight or tail suspension fibers. Moreover, although hexokinase on average increased significantly in all four fiber groups (Figs. 5 and 6), the range of activities did not increase above the synchronous range of less than 2. Note how few F or T fibers remained within the soleus boundary for the two enzymes. To anticipate the results with TA fibers, hexokinase levels did not correlate with fiber size.

Individual KACAT activities did not correlate positively or negatively with hexokinase or with any of the other enzymes measured.

TIBIALIS ANTERIOR MUSCLE

Average values.

Most of the soleus fibers are slow-twitch (Type 1), therefore the relatively few fibers that it is practicable to analyze individually should furnish a reasonable indication of the composition of the muscle as a whole. This is not true for TA muscles which contain two distinct fiber types that are non-uniformly distributed among different regions of the muscle. Therefore, although an attempt was made to choose fibers at random, there can be no assurance that the 20 or so fibers analyzed from each muscle were truly representative of the muscle as a whole. The average values in Table 2 should consequently be evaluated with this in mind.

It is rather clear that in contrast to the soleus fibers, there was no major change in fiber size (dry weight per unit length) related to flight or tail suspension. This fits with the lack of substantial difference in total wet weight of the muscles from which these TA fibers came.

In contrast to the results for soleus fibers there were only two statistically significant differences ($P < 0.05$) between TA enzyme activities for synchronous fibers and those of either flight or tail suspension TA fibers: Hexokinase activity of T7 averaged 57% higher than the average for S7, the higher of the two synchronous sets; thiolase activity of F7 was 27% lower than the average for S6, the lower of the two synchronous fiber sets.

Individual TA fiber values.

Examination of the data on a fiber-by-fiber basis shows some interesting relationships between different enzymes and between size and enzyme activities, as well as some effects of flight and tail suspension obscured by averaging all the data.

Figs. 7-9 show the rather striking negative correlation between fiber size and malate dehydrogenase (MDH) which applies as well to synchronous (Fig. 7) flight (Fig. 8) tail suspension (Fig. 9) fibers. Note that almost all of the values from F6, F7, T6 and T7 fall within the S6 plus S7 domain or close by. The correlation coefficients between size and MDH ranged from -0.603 for F7 to -0.915 for S7 ($P < 0.01$ in all cases).

Hexokinase and MDH activities were closely correlated, and in the synchronous and flight data could be almost superimposed (Fig. 10). The correlation coefficients were all very high: 0.946 (S6), 0.985 (S7), 0.890 (F6), 0.890 (F7). There was no sign of any important differences in the range of values. In contrast, among the tail suspension fibers (Fig. 11), although hexokinase and MDH were also tightly correlated for T6 and T7 ($r = 0.951$ and 0.861 respectively), the slope of the regression lines were much steeper than for S6 and S7. Consequently, the hexokinase to MDH ratios were very similar at the low end of the MDH scale and much higher at the upper end. Clearly, there had been relative increases in hexokinase among TA fibers with high MDH from both T6 and T7, but the increase in T6 was obscured in Table 2 because fibers with low MDH had predominated either in the original selection or in the muscle as a whole.

Figs. 12 and 13 bring out another aspect of the increase in hexokinase which took place in the tail suspension fibers. In the control (S6 and S7) fibers hexokinase and size were closely correlated (Fig. 12) as might have been expected ($r = -0.733$ and -0.920 for S6 and S7 respectively). However, in the case of T6 and T7, the relationship between size and hexokinase ceased with hexokinase activities greater than control (Fig. 13).

Pyruvate kinase and hexokinase activities in TA fibers proved to be negatively correlated (Figs. 4-6), in contrast to the positive correlation seen in the same figures for soleus fibers. There was little change in the distribution among the flight fibers except for one fiber from each muscle which drifted toward the soleus region in regard to pyruvate kinase. The increases in hexokinase activity among the tail suspension fibers were clearly much larger for those with lowest pyruvate kinase activity, just as they had been larger for fibers with highest MDH activity.

Thiolase was closely correlated with both MDH and hexokinase. A plot of hexokinase against thiolase (not shown) was almost indistinguishable from that against MDH (Fig. 10) with r values ranging from 0.813 to 0.980. As expected, thiolase is negatively correlated with pyruvate kinase (Fig. 14). Only the 15 out of 36 flight and tail suspension fibers which fell outside the S6 and S7 zone are indicated. There seems to be no specific trend in these deviations from S6 and S7.

Phosphoglucoisomerase correlated well with pyruvate kinase among individual fibers but there were no substantial differences between synchronous, flight, and tail suspension muscles in the interrelationships or range of values (data not shown).

Relationship of enzyme levels to myosin ATPase fiber types.

Table 3 records activities of phosphofructokinase (PFK) and GOPDH in fibers from S7, F7, and T7 identified as to fiber type by staining for myosin ATPase. PFK was significantly higher in type 1 and 2B fibers from F7 than from S7 (+58% and +31% respectively). PFK was also 27% higher in F7, 2A fibers but the difference was not statistically significant. GOPDH, however, was significantly higher in 2A and 2B fibers of both F7 and T7 fibers by significant amounts (respectively, 162% and 88% higher in 2A and 2B fibers of F7, and 88% and 47% higher in 2A and 2B fibers of T7). Fig. 15 displays the relationships between PFK and GOPDH among individual fibers analyzed for both enzymes. Note that the GOPDH levels of all 2B fibers from each muscle (S7, F7 or T7) are higher than the level in any 2A fiber from the same muscle.

MDH and glycogen phosphorylase were also measured in fibers typed for myosin ATPase (Table 4, Fig. 16). Only in one case was a statistically significant difference related to flight or tail suspension observed among the average values (Table 3). Average phosphorylase activity in T7 2B fibers was 24% higher than in S7, and 41% higher than in F7. The plot of MDH against phosphorylase (Fig. 16) shows complete separation of MDH activities of 2A and 2B fibers of all three muscles, and only a slight overlap of phosphorylase activities which was limited to F7 fibers. A few 2C fibers were identified and assayed from the F7 muscle. Their MDH activities overlapped completely with type 1 fibers and their phosphorylase levels were on the average 18% lower, but the difference was not statistically significant.

TABLE 1. SIZE AND LEVELS OF FIVE ENZYMES IN INDIVIDUAL SOLEUS FIBERS

Rat	Size	Pyruvate kinase	Hexokinase	KACAT	GOPDH	P-fructokinase
	(μg/mm)	(mol h^{-1} kg^{-1} (dry) at 20°C)				
S6	0.705 ± .021 CV 12%	11.7 ± 0.8 28%	0.388 ± .017 17%	0.478 ± .014 12%	0.43 ± .04 35%	
S7	0.818 ± .041 CV 20%	11.5 ± 1.0 35%	0.506 ± .020 16%	0.470 ± .016 14%	0.43 ± .04 37%	3.52 ± .28 32%
F6	0.545* ± .033 CV 24%	16.6 ± 2.6 63%	0.602* ± .013 9%	0.421* ± .018 17%	0.71* ± .10 60%	
F7	0.393* ± .029 CV 30%	16.0* ± 1.8 45%	0.716* ± .026 15%	0.423* ± .016 15%	0.63* ± .10 57%	4.46 ± .48 40%
T6	0.491* ± .024 CV 19%	26.2* ± 3.9 57%	0.587* ± .023 15%	0.372* ± .022 23%	0.97* ± .14 52%	
T7	0.470* ± .018 CV 15%	12.4 ± 0.9 30%	0.929* ± .024 10%	0.463 ± .012 10%	0.62* ± .06 40%	4.17 ± .45 43%

Each entry is the average for the same 16 fibers (15 for T6) analyzed in duplicate, ± S.E.. Abbreviations are KACAT, 3-ketoacid CoA transferase; GOPDH, glycerol-3-phosphate dehydrogenase; and CV, coefficient of variation. An asterisk indicates a significant difference ($P \leq 0.05$) from both S6 and S7.

TABLE 2. SIZE AND LEVELS OF FIVE ENZYMES IN INDIVIDUAL TA MUSCLE FIBERS

Rat		Size	MDH	HK	Thiolase	PK	PGI
S6		0.641	12.4	0.387	1.35	81.4	69.2
(23)	S.E.	± .035	± 1.1	± .026	± .13	± 5.3	± 2.6
	CV	26%	43%	32%	46%	20%	11%
S7		0.790	13.9	0.543	1.53	89.2	64.2
(23)	S.E.	± .061	± 1.6	± .053	± .21	± 9.3	± 3.3
	CV	37%	55%	47%	66%	31%	15%
F6		0.615	14.2	0.533	1.49	90.3	73.5
(22)	S.E.	± .031	± 1.0	± .031	± .17	± 7.7	± 4.4
	CV	24%	33%	27%	54%	26%	18%
F7		0.634	12.7	0.499	0.98*	92.7	66.2
(21)	S.E.	± .035	± 1.1	± .038	± .12	± 9.7	± 5.1
	CV	25%	40%	35%	56%	31%	23%
T6		0.749	11.6	0.546	1.00	91.6	71.6
(23)	S.E.	± .039	± 1.3	± .061	± .16	± 8.2	± 3.2
	CV	25%	54%	54%	77%	27%	13%
T7		0.624	12.1	0.850*	1.47	95.6	69.3
(24)	S.E.	± .042	± 1.2	± .120	± .17	± 7.1	± 3.4
	CV	33%	49%	69%	57%	22%	15%

Activities are recorded as in Table 1, ± S.E. for the number of fibers given in parentheses in the left hand column, except that pyruvate kinase (PK) and phosphoglucoisomerase (PGI) are for only 9 fibers from each muscle. An asterisk indicates a significant difference ($P < 0.05$) from both S6 and S7.

TABLE 3. PHOSPHOFRUCTOKINASE (PFK) AND GLYCERO-DEHYDROGENASE (GOPDH) IN TIBIALIS ANTERIOR FIBERS TYPED BY STAINING FOR MYOSIN ATPase

Fiber Type	Phosphofructokinase			Glycerol-P dehydrogenase		
	S7	F7	T7	S7	F7	T7
1	1.99 (3)	3.15 (4)*				
	S.E. ± .38	± .27				
	CV 33%	17%				
2A	5.08 (10)	6.43 (10)	5.24 (9)	0.85 (7)	2.23 (6)*	1.60 (6)*
	S.E. ± .51	± .49	± .41	± .18	± .19	± .25
	CV 31%	24%	23%	56%	21%	38%
2B	7.64 (8)	10.0 (10)*	8.6 (12)	2.03 (8)	4.52 (9)*	2.99 (12)*
	S.E. ± .58	± .43	± .42	± .12	± .20	± .16
	CV 21%	14%	15%	17%	13%	19%

Activities are mol h^{-1} kg^{-1} (dry wt) at 20°C ± S.E. for the number of samples in parentheses. Asterisks indicate a statistically significant difference from the corresponding S7 value ($P \leq 0.05$).

TABLE 4. MALATE DEHYDROGENASE AND PHOSPHORYLASE IN TIBIALIS ANTERIOR FIBERS TYPED BY STAINING FOR MYOSIN ATPase

Fiber Type	Malate dehydrogenase			Phosphorylase		
	S7	F7	T7	S7	F7	T7
1	12.1 (5)	12.4 (4)	13.7 (6)	1.19 (5)	0.97 (4)	1.09 (6)
	S.E. ± .6	± .41	± 1.6	± .14	± .13	± .10
	CV 11%	7%	28%	25%	27%	23%
2C		14.2 (7)			0.80 (7)	
	S.E.	± 1.06			± .06	
	CV	20%			20%	
2A	14.5(8)	15.5 (7)	17.0 (6)	2.65 (8)	3.01 (7)	2.50 (6)
	S.E. ± 1.3	± 1.4	± 1.0	± .16	± .25	± .22
	CV 26%	23%	14%	18%	22%	21%
2B	4.11 (7)	4.79 (9)	4.85 (10)	4.98 (7)	4.38 (9)	6.17 (10)*
	S.E. ± .35	± .39	± .21	± .24	± .27	± .39
	CV 23%	24%	14%	13%	16%	20%

Activities recorded as in Table 1 for the number of fibers given in parentheses. An asterisk (*) indicates a significant difference from the corresponding S7 value.

FIG. 1

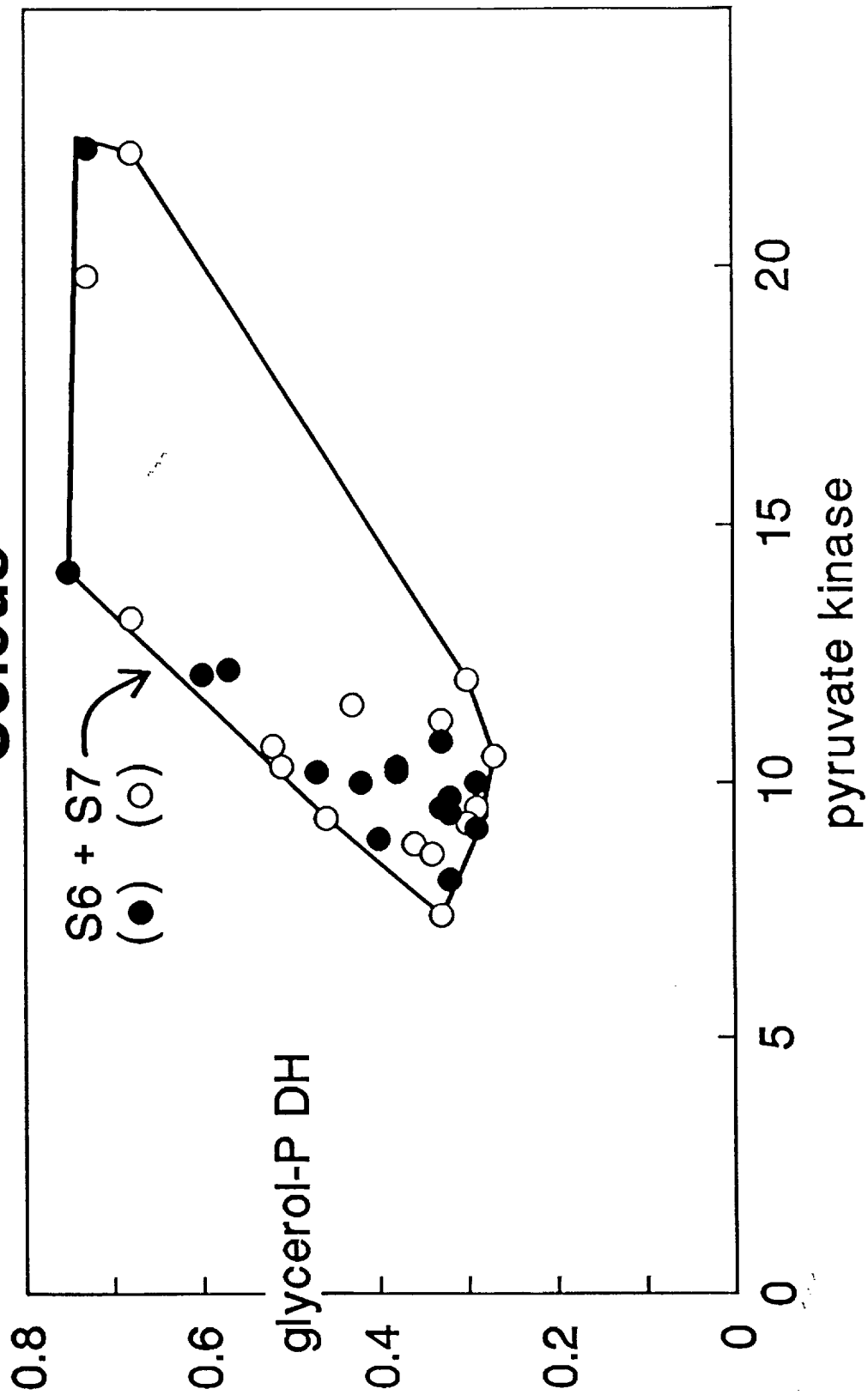
Soleus
S6 + S7
(●) (○)
glycerol-P DH
pyruvate kinase
0.8
0.6
0.4
0.2
0
0
5
10
15
20

FIG. 2

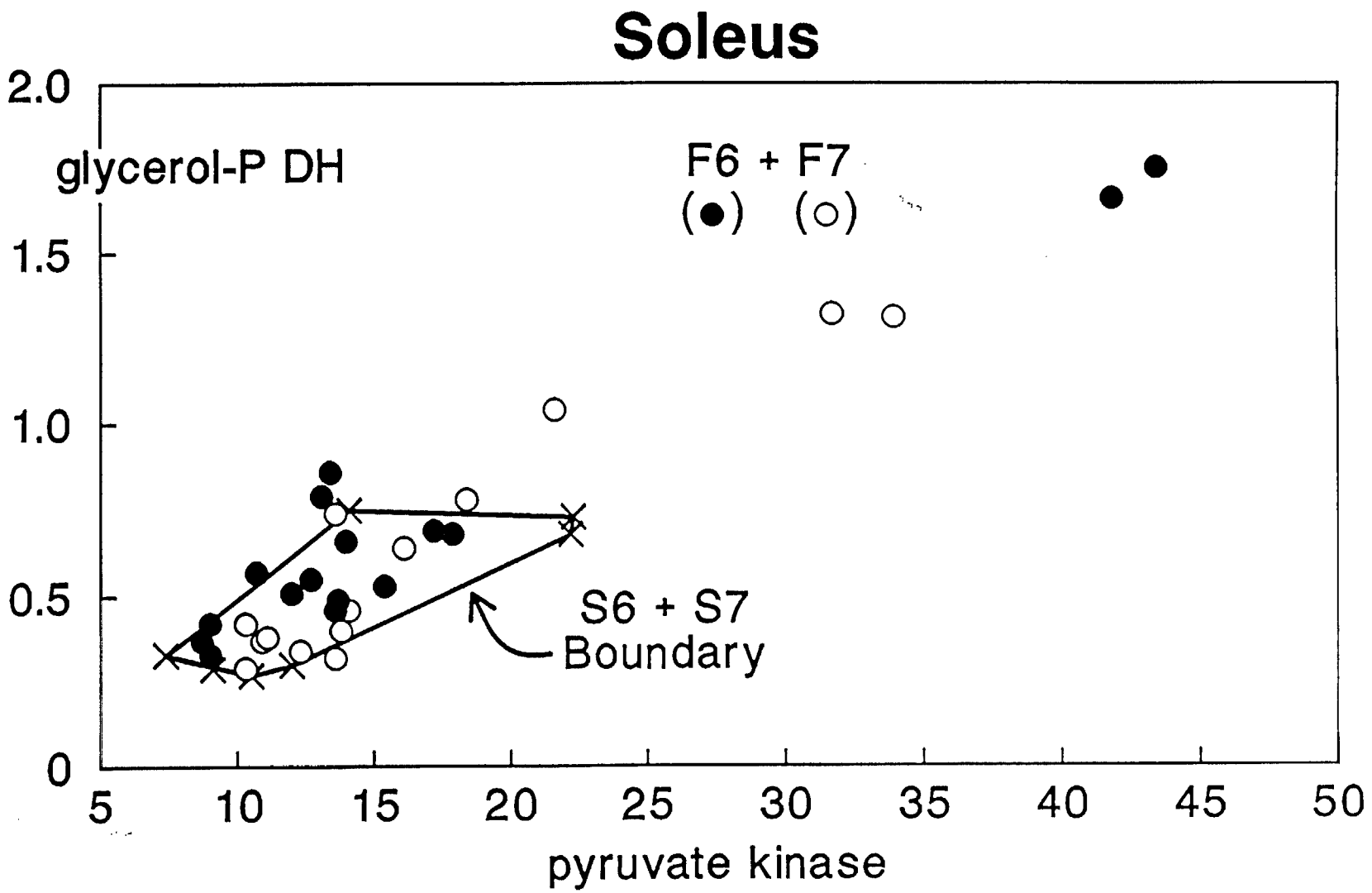
Soleus
2.0
glycerol-P DH
F6 + F7
(●) (○)
1.5
1.0
0.5
0
S6 + S7
Boundary
5
10
15
20
25
30
35
40
45
50
pyruvate kinase

FIG. 3

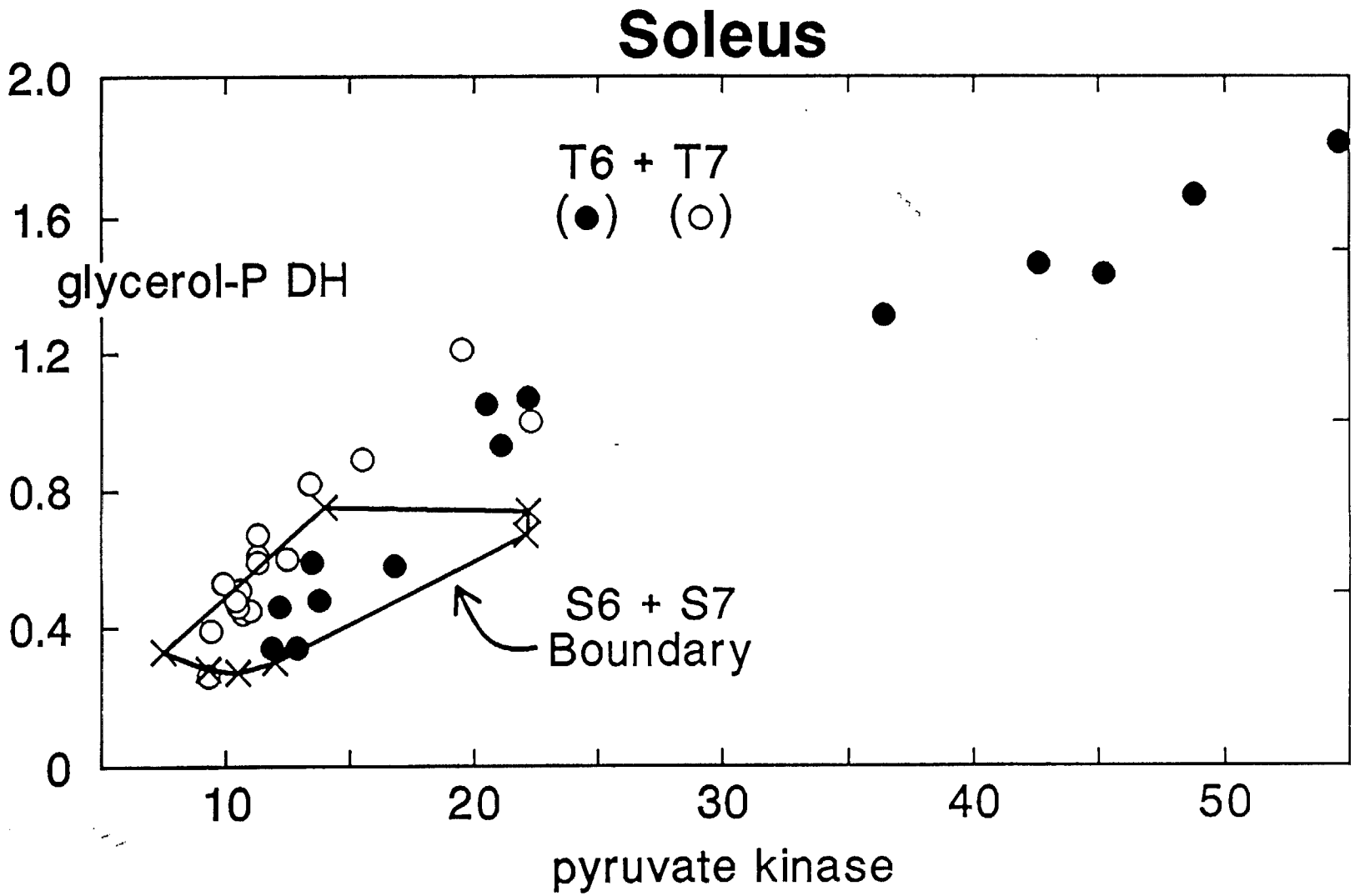
Soleus
2.0
1.6
1.2
0.8
0.4
0
glycerol-P DH
T6 + T7
(●) (○)
S6 + S7
Boundary
10
20
30
40
50
pyruvate kinase

FIG. 4

Fig 4

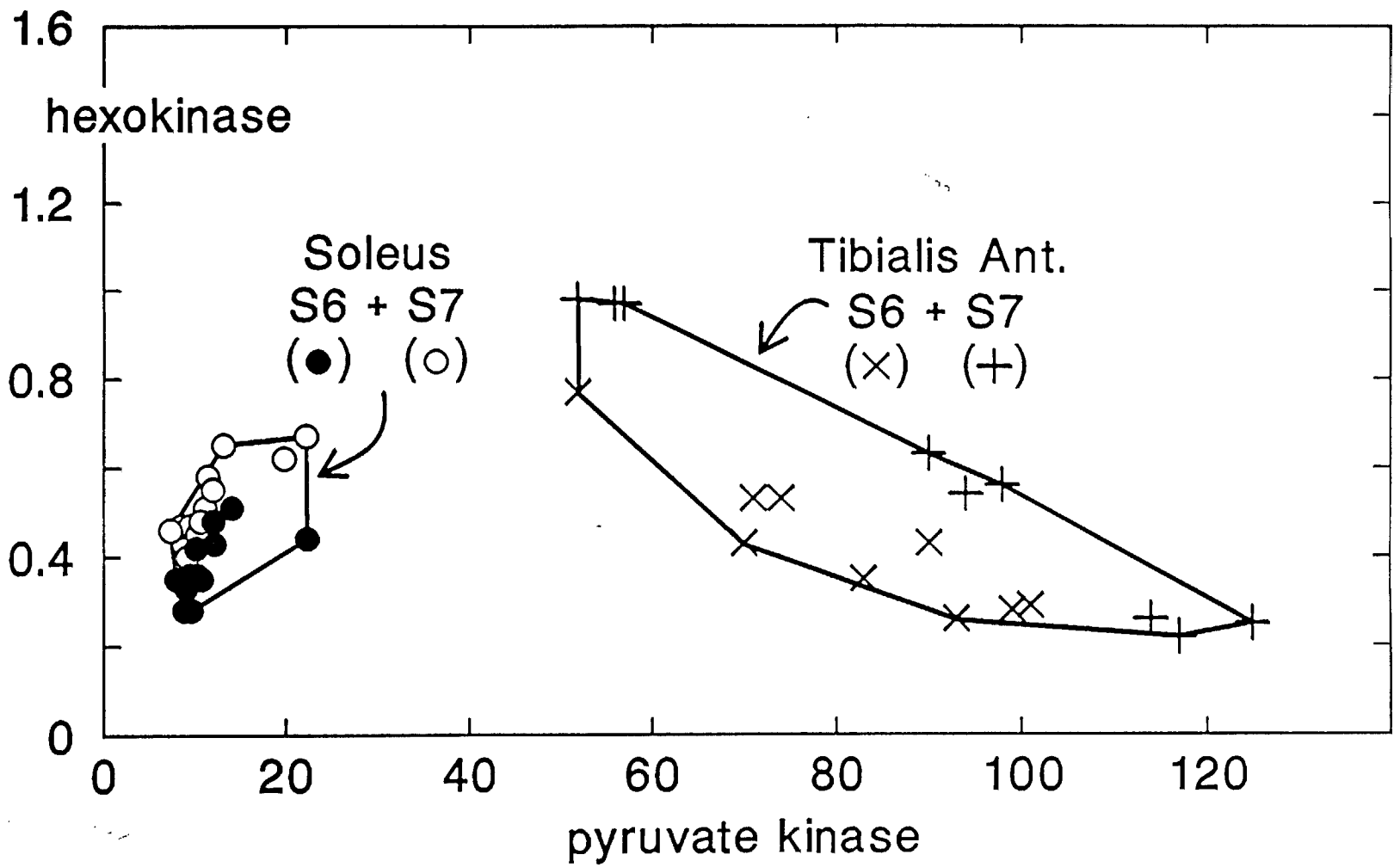
1.6
hexokinase
1.2
0.8
0.4
0
Soleus
S6 + S7
(●) (○)
Tibialis Ant.
S6 + S7
(×) (+)
0
20
40
60
80
100
120
pyruvate kinase

FIG. 5

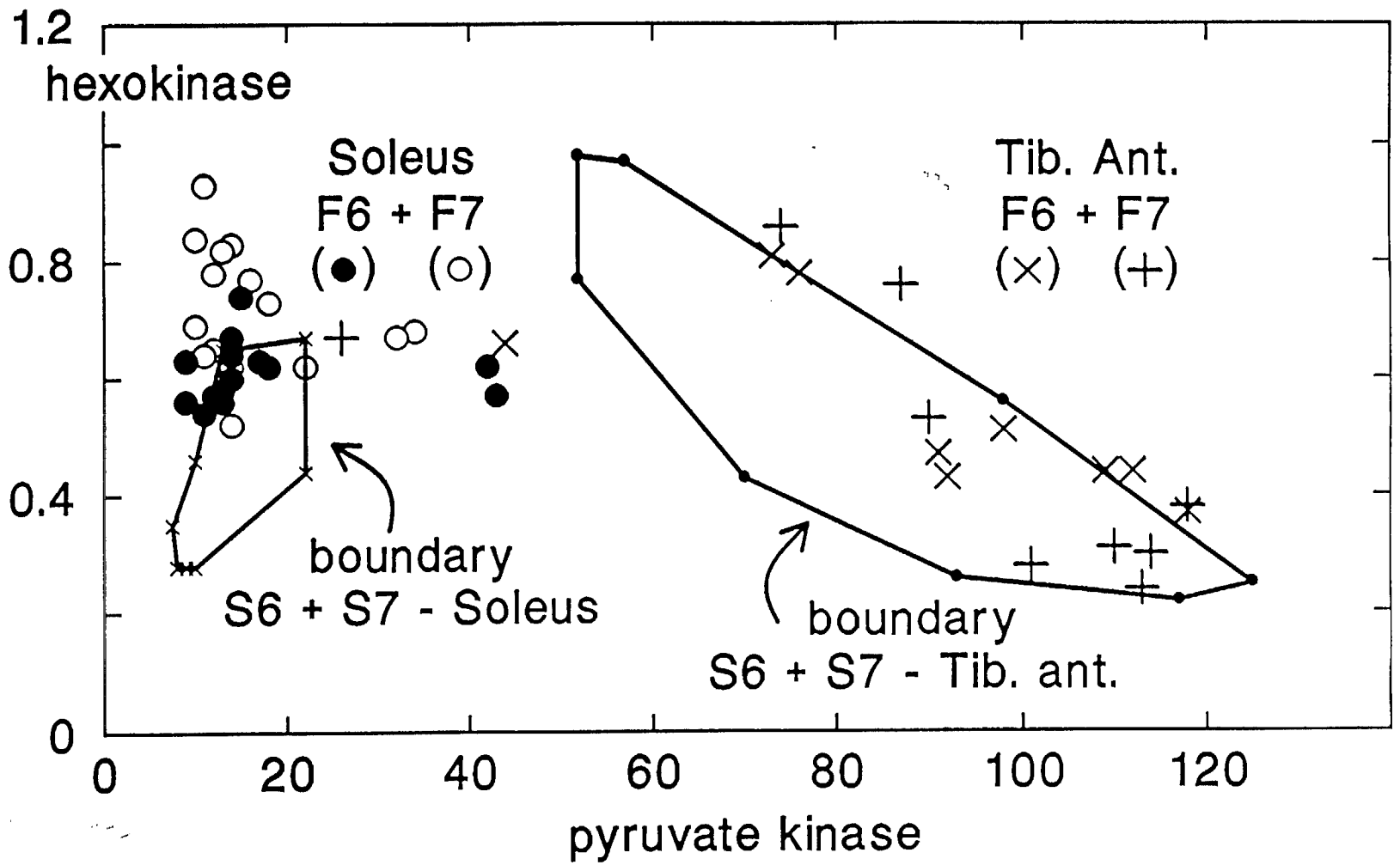
1.2
hexokinase
0.8
0.4
0
0
20
40
60
80
100
120
pyruvate kinase
Soleus
F6 + F7
(●) (○)
Tib. Ant.
F6 + F7
(×) (+)
boundary
S6 + S7 - Soleus
boundary
S6 + S7 - Tib. ant.

FIG. 6

Fig 6

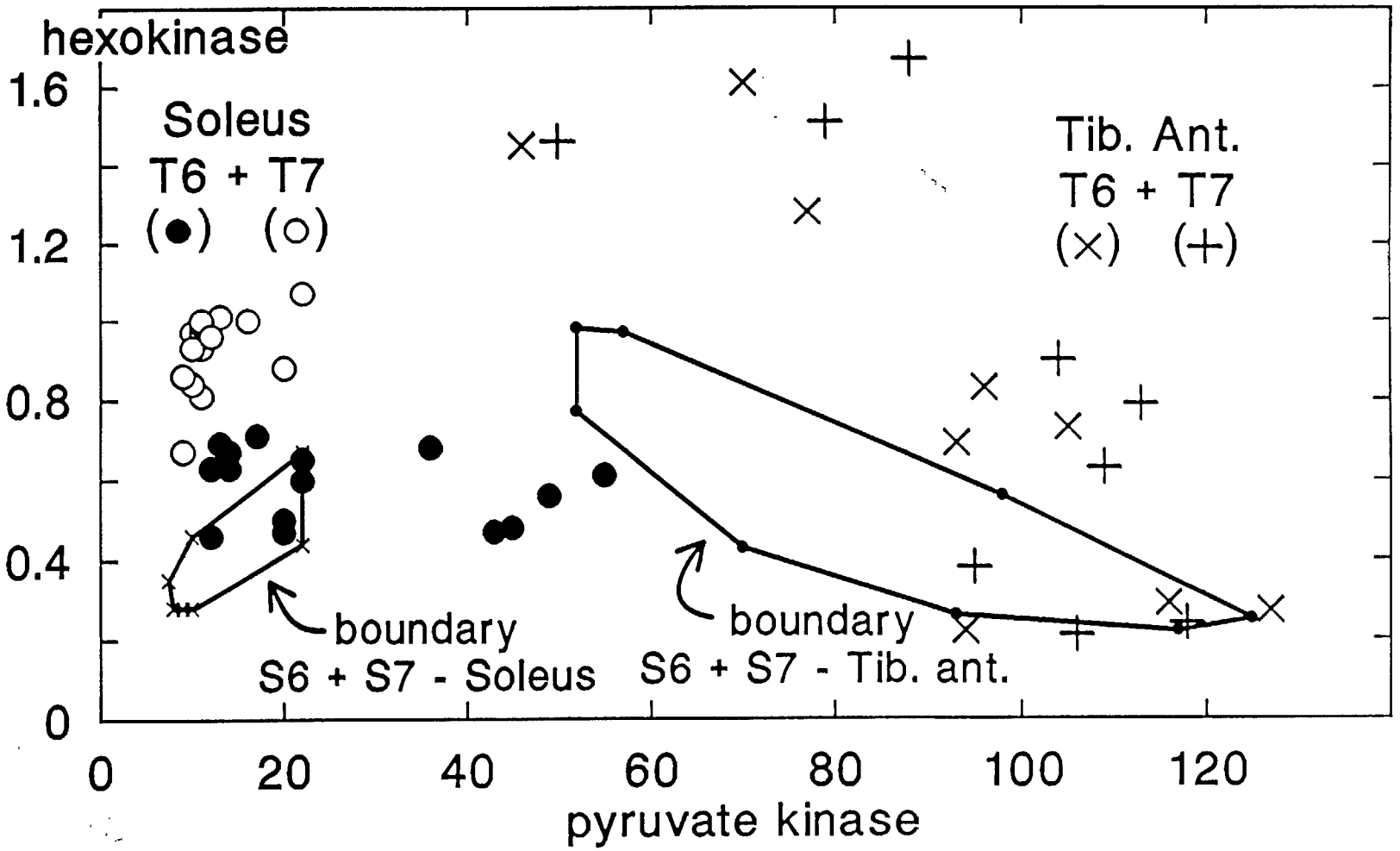
hexokinase
1.6
1.2
0.8
0.4
0
Soleus
T6 + T7
(●) (○)
Tib. Ant.
T6 + T7
(×) (+)
boundary
S6 + S7 - Soleus
boundary
S6 + S7 - Tib. ant.
0
20
40
60
80
100
120
pyruvate kinase

FIG. 7 Fig 7

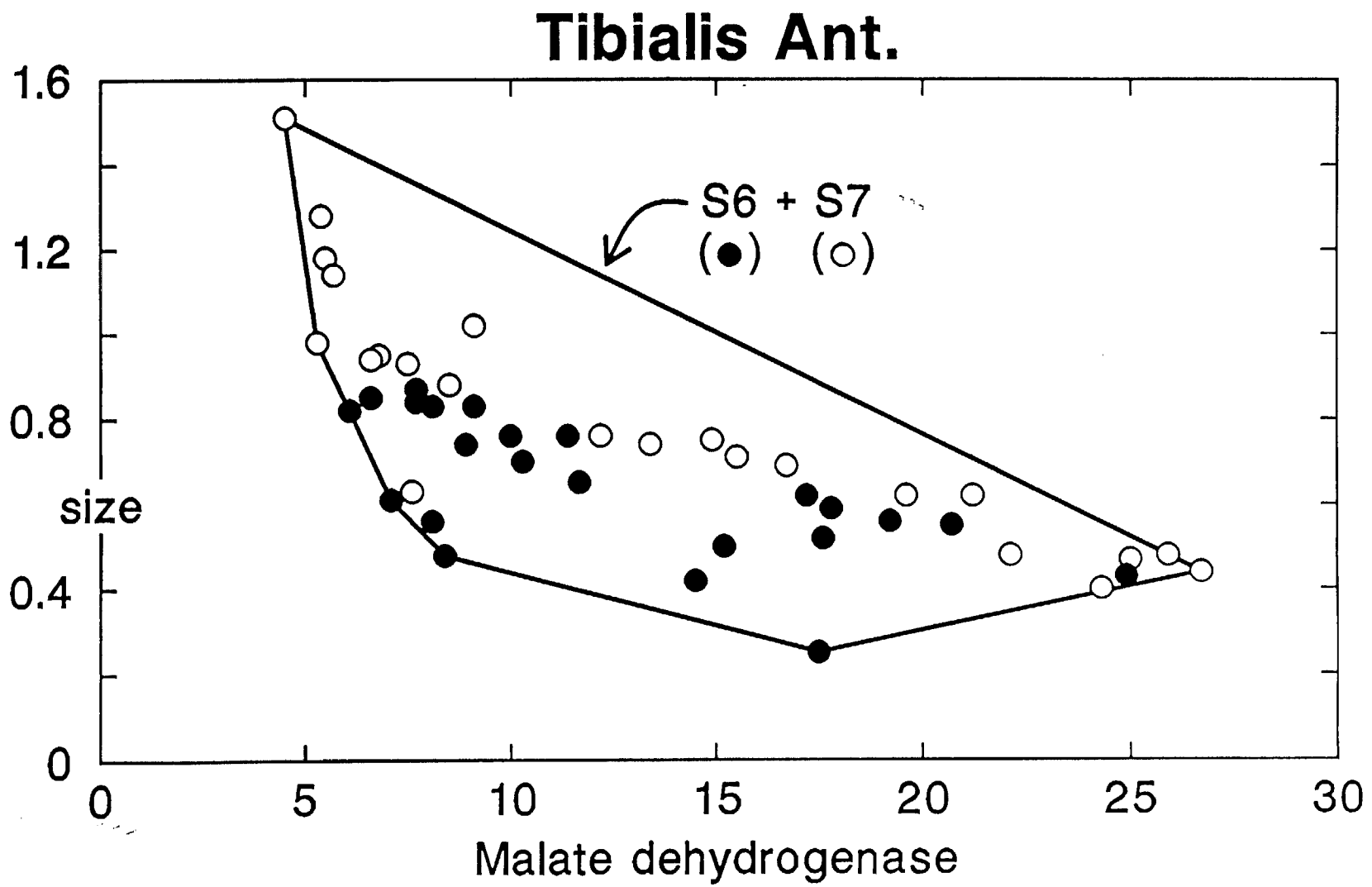
Tibialis Ant.
1.6
1.2
0.8
0.4
0
size
S6 + S7
(●) (○)
0
5
10
15
20
25
30
Malate dehydrogenase

FIG. 8

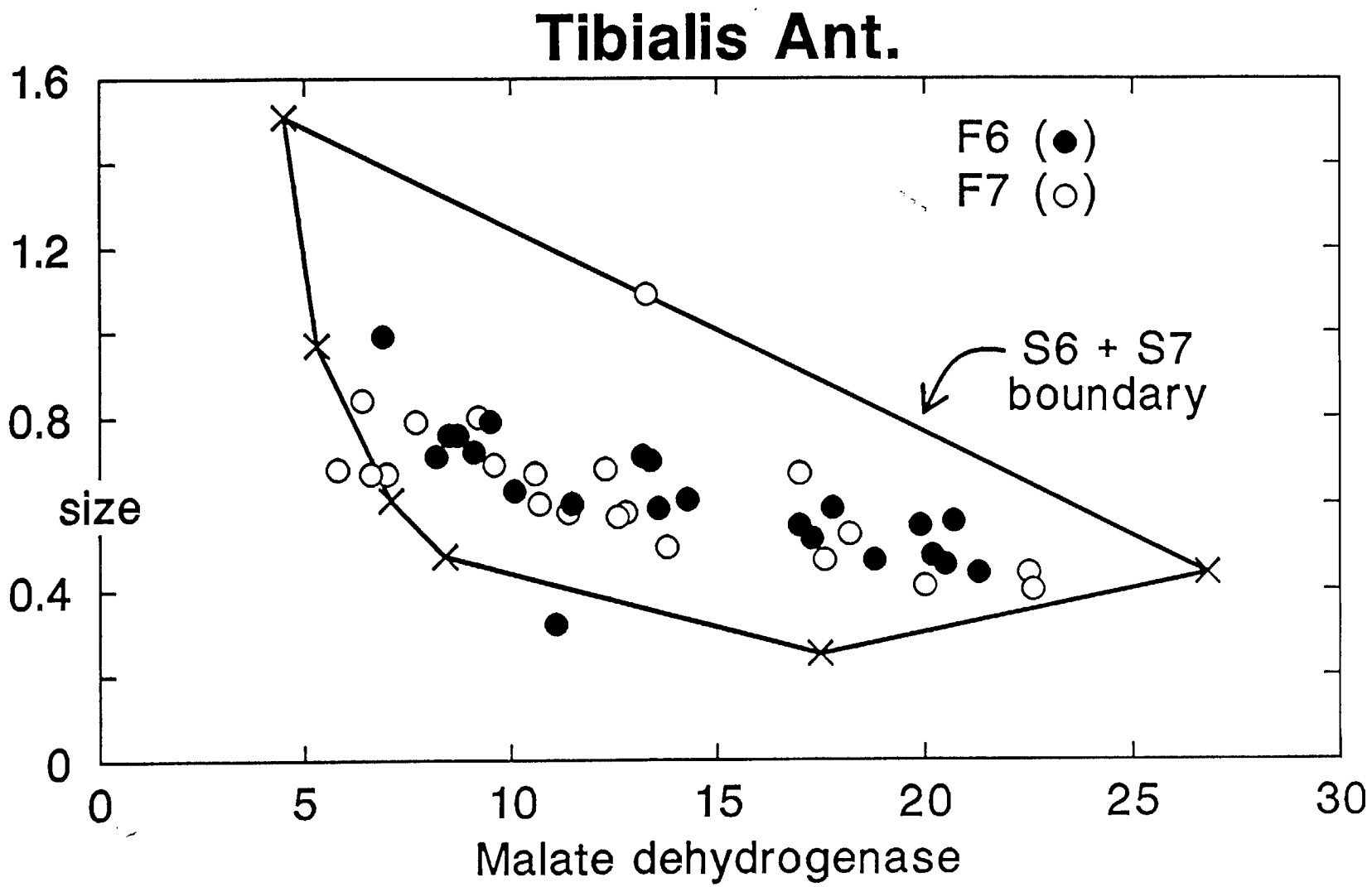
Tibialis Ant.
F6 (●)
F7 (○)
S6 + S7
boundary
size
1.6
1.2
0.8
0.4
0
0
5
10
15
20
25
30
Malate dehydrogenase

FIG. 9 Fig 9

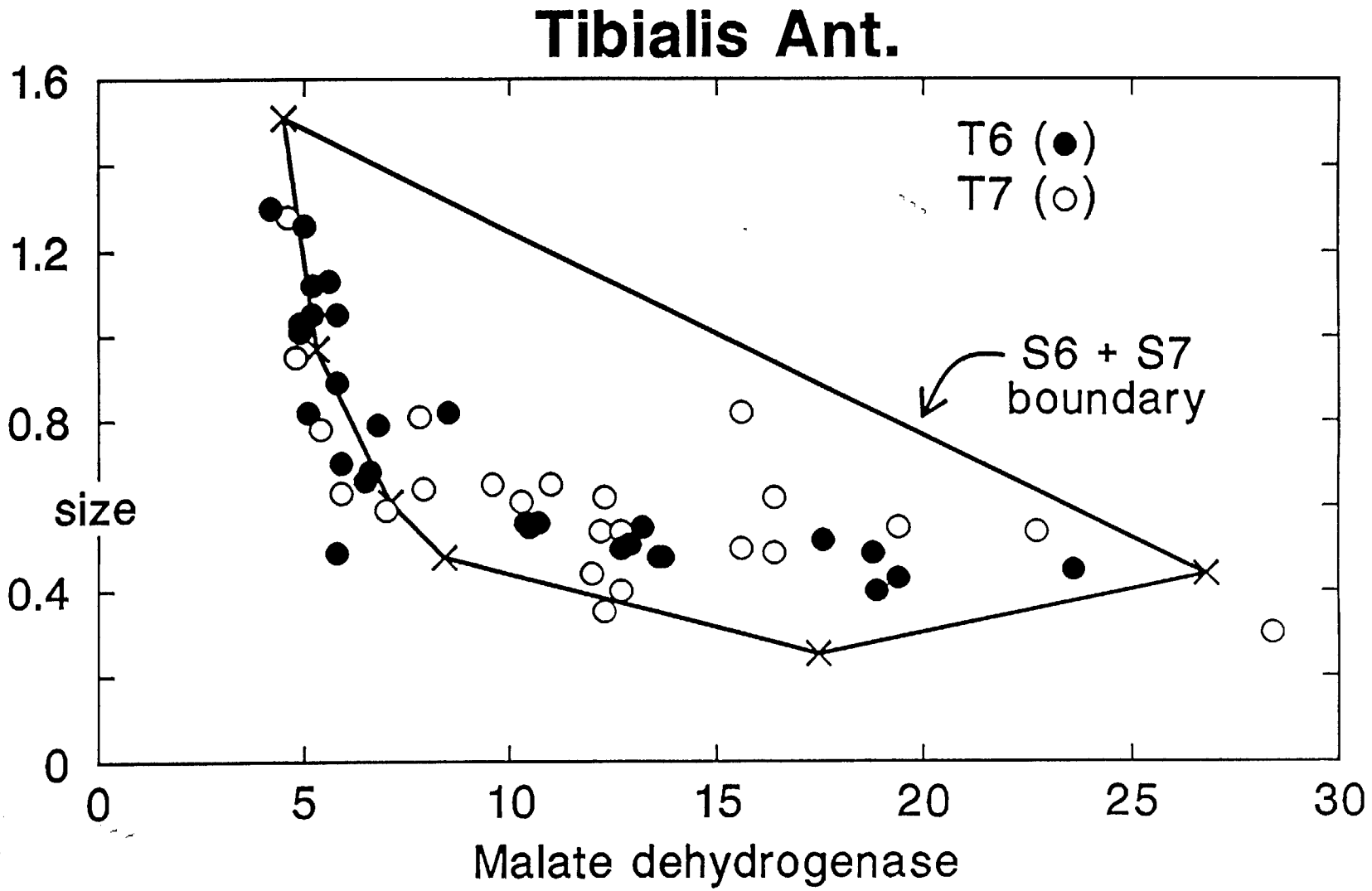
Tibialis Ant.
T6 (●)
T7 (○)
S6 + S7
boundary
size
1.6
1.2
0.8
0.4
0
0
5
10
15
20
25
30
Malate dehydrogenase

FIG. 10

Fig 10

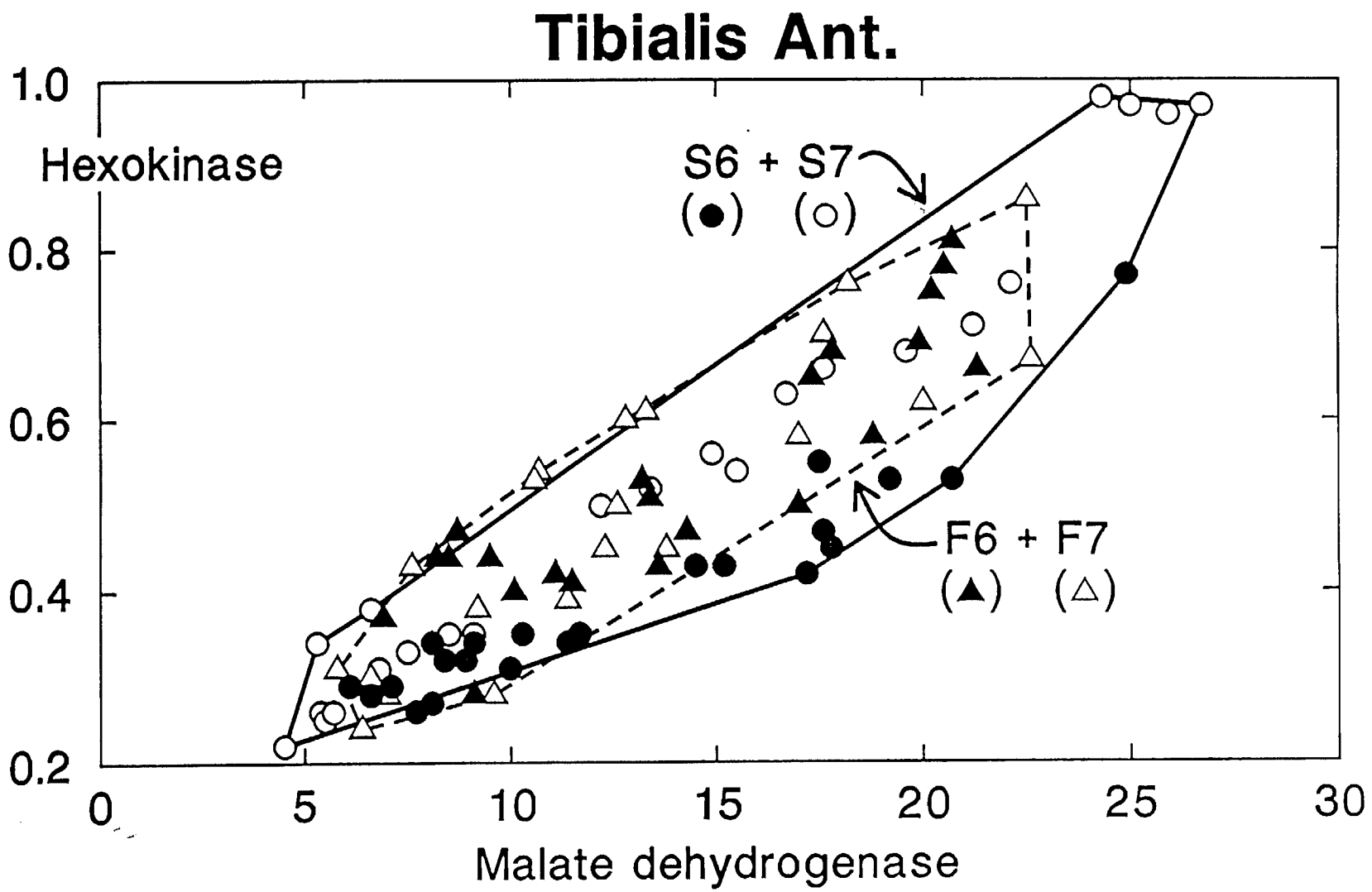
Tibialis Ant.
Hexokinase
1.0
0.8
0.6
0.4
0.2
0
5
10
15
20
25
30
Malate dehydrogenase
S6 + S7
(●) (○)
F6 + F7
(▲) (△)

FIG. 11

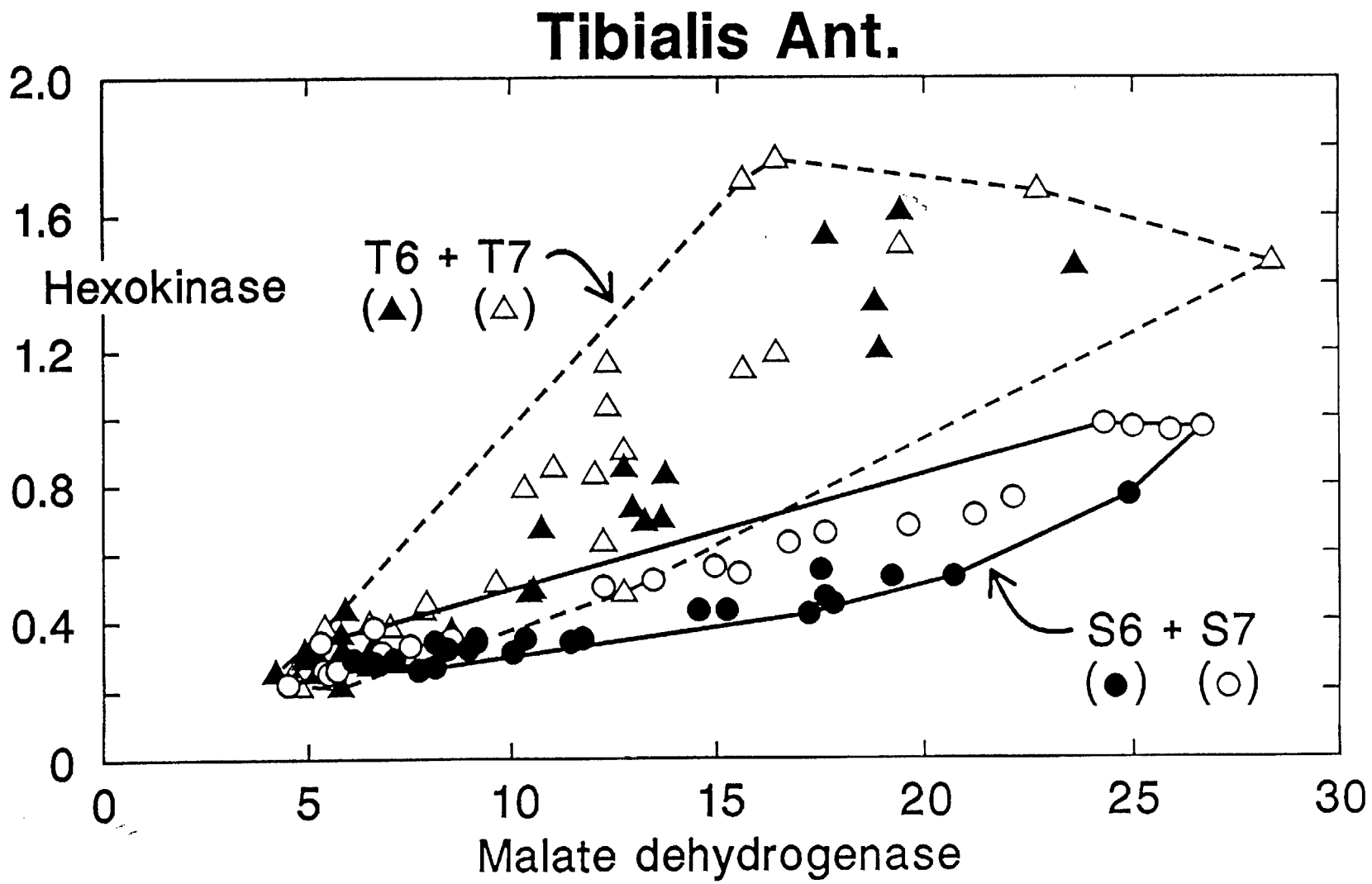
Tibialis Ant.
2.0
1.6
1.2
0.8
0.4
0
Hexokinase
T6 + T7
(▲) (△)
S6 + S7
(●) (○)
0
5
10
15
20
25
30
Malate dehydrogenase

FIG. 12

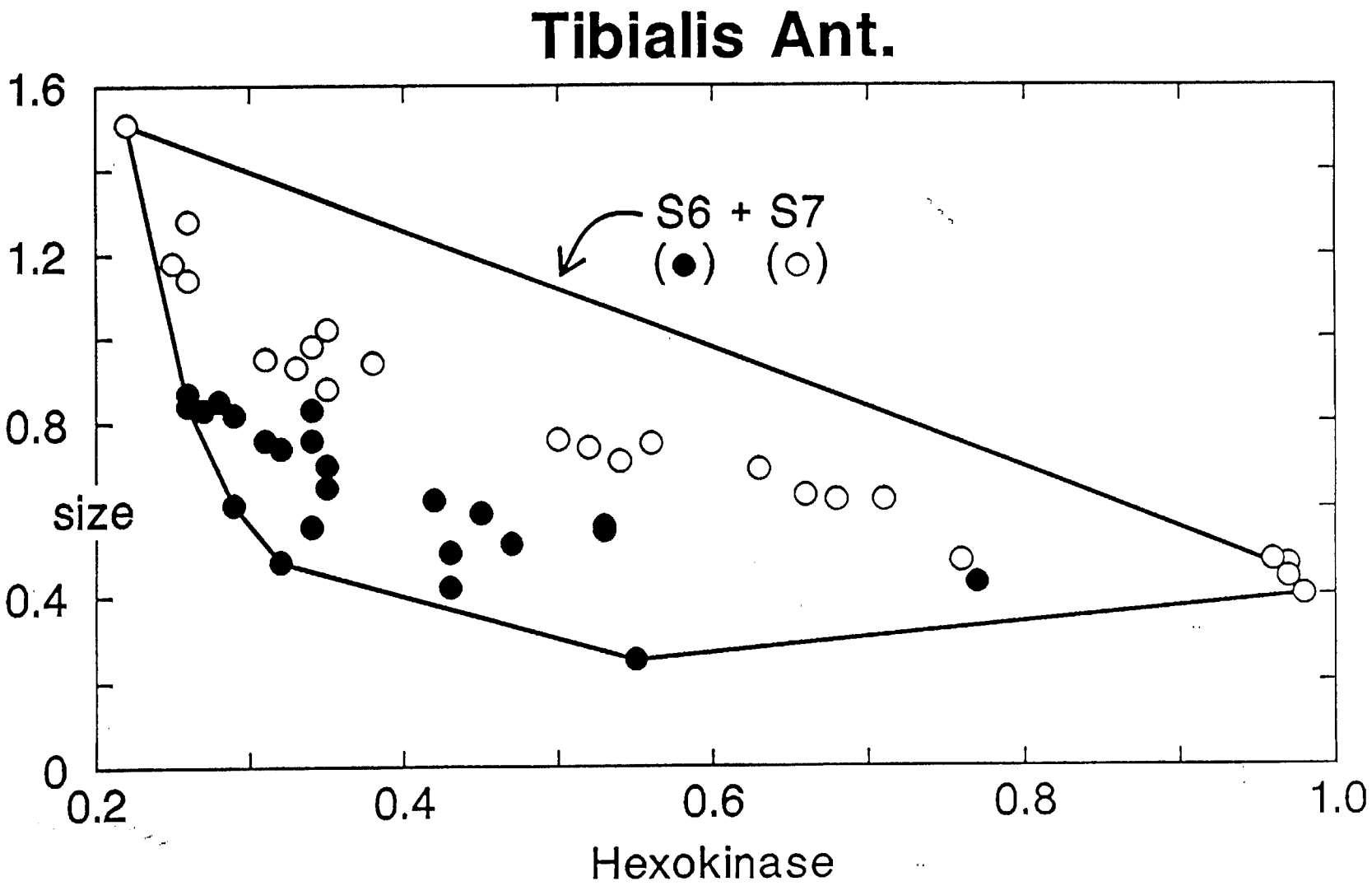

FIG. 13

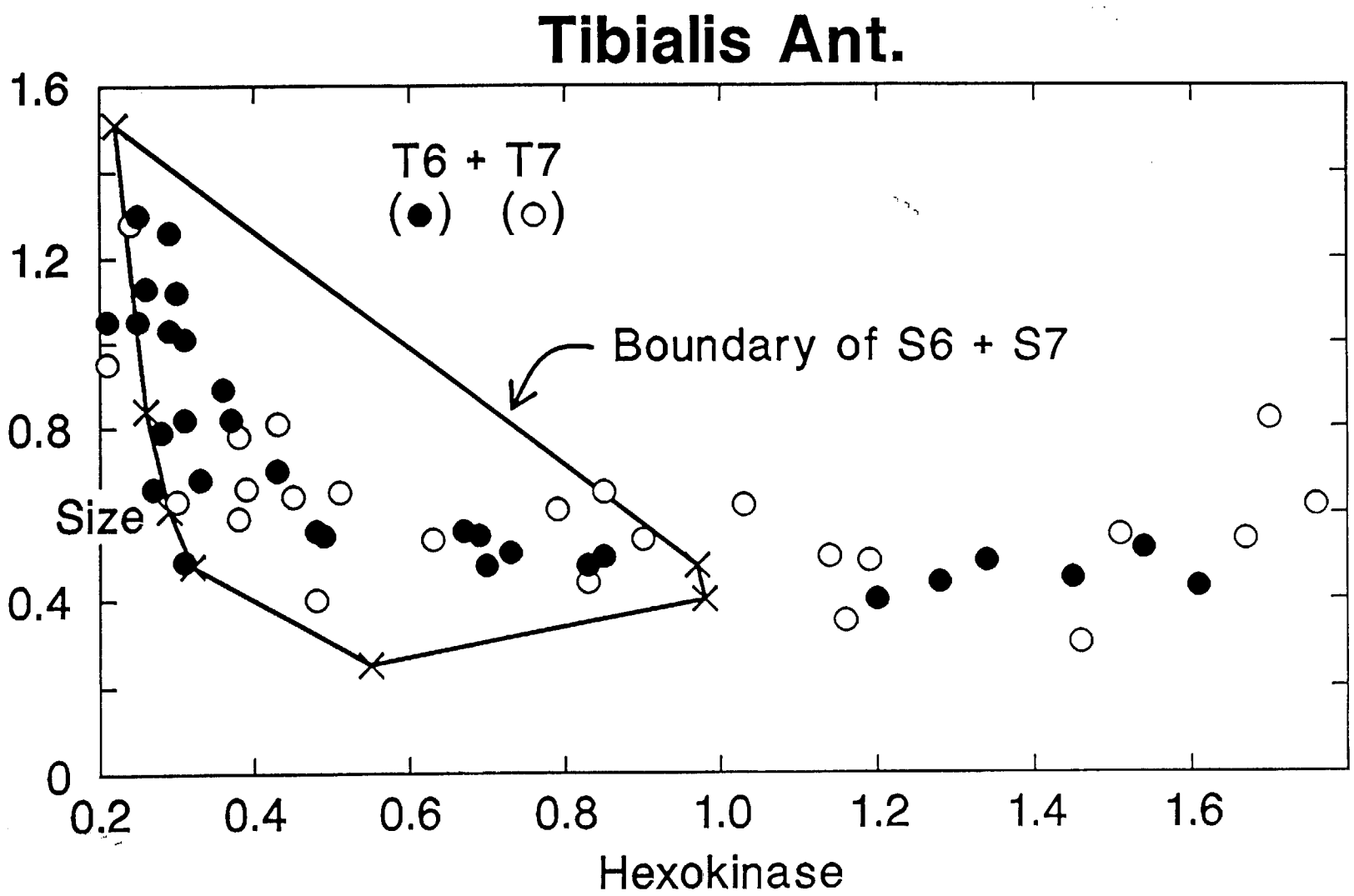
Tibialis Ant.
T6 + T7
(●) (○)
Boundary of S6 + S7
Size
1.6
1.2
0.8
0.4
0
0.2
0.4
0.6
0.8
1.0
1.2
1.4
1.6
Hexokinase

FIG. 14

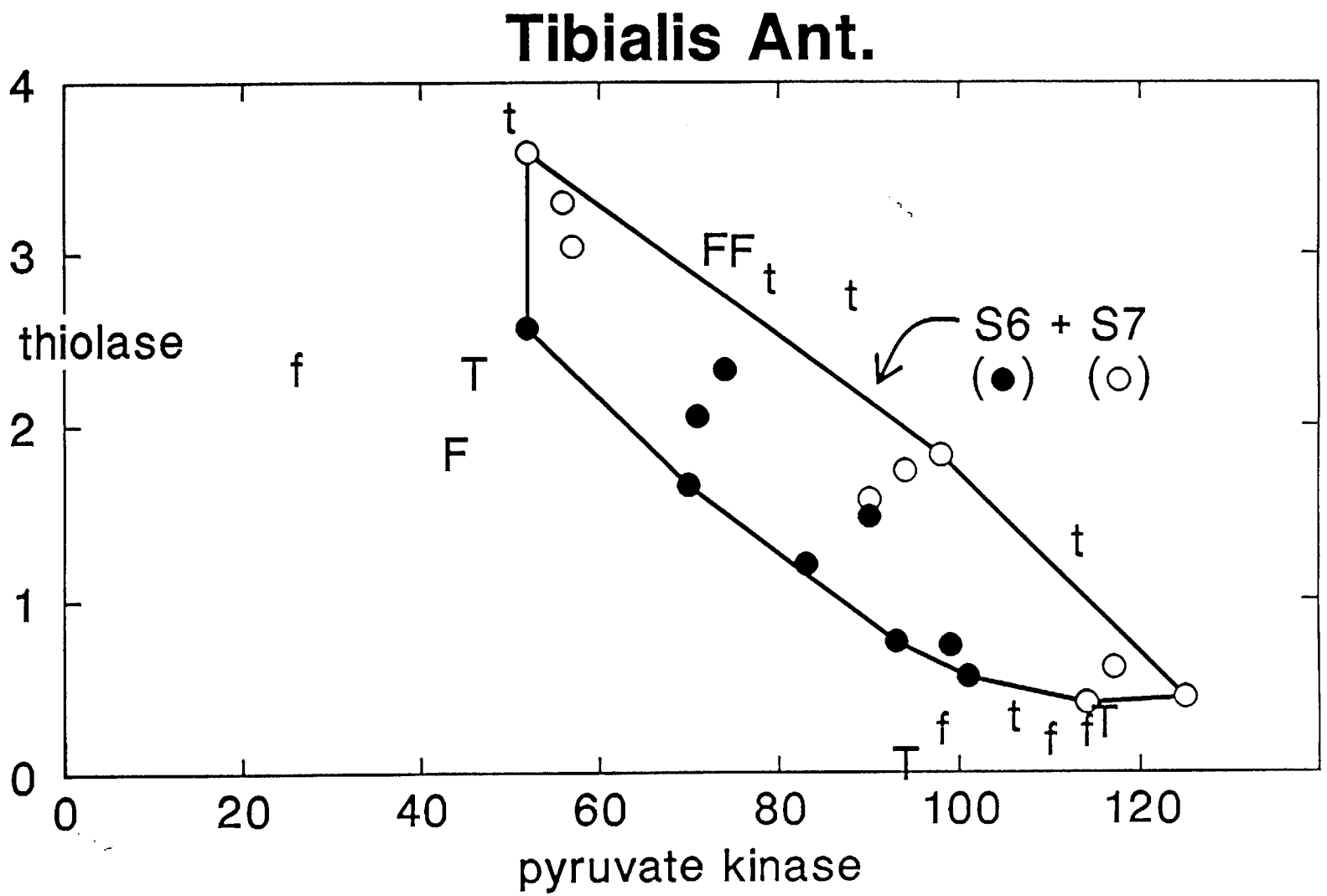
Tibialis Ant.
thiolase
pyruvate kinase
0
1
2
3
4
0
20
40
60
80
100
120
t
FF
t
t
S6 + S7
(●) (○)
f
T
F
t
t
f
t
f
fT
T

FIG. 15

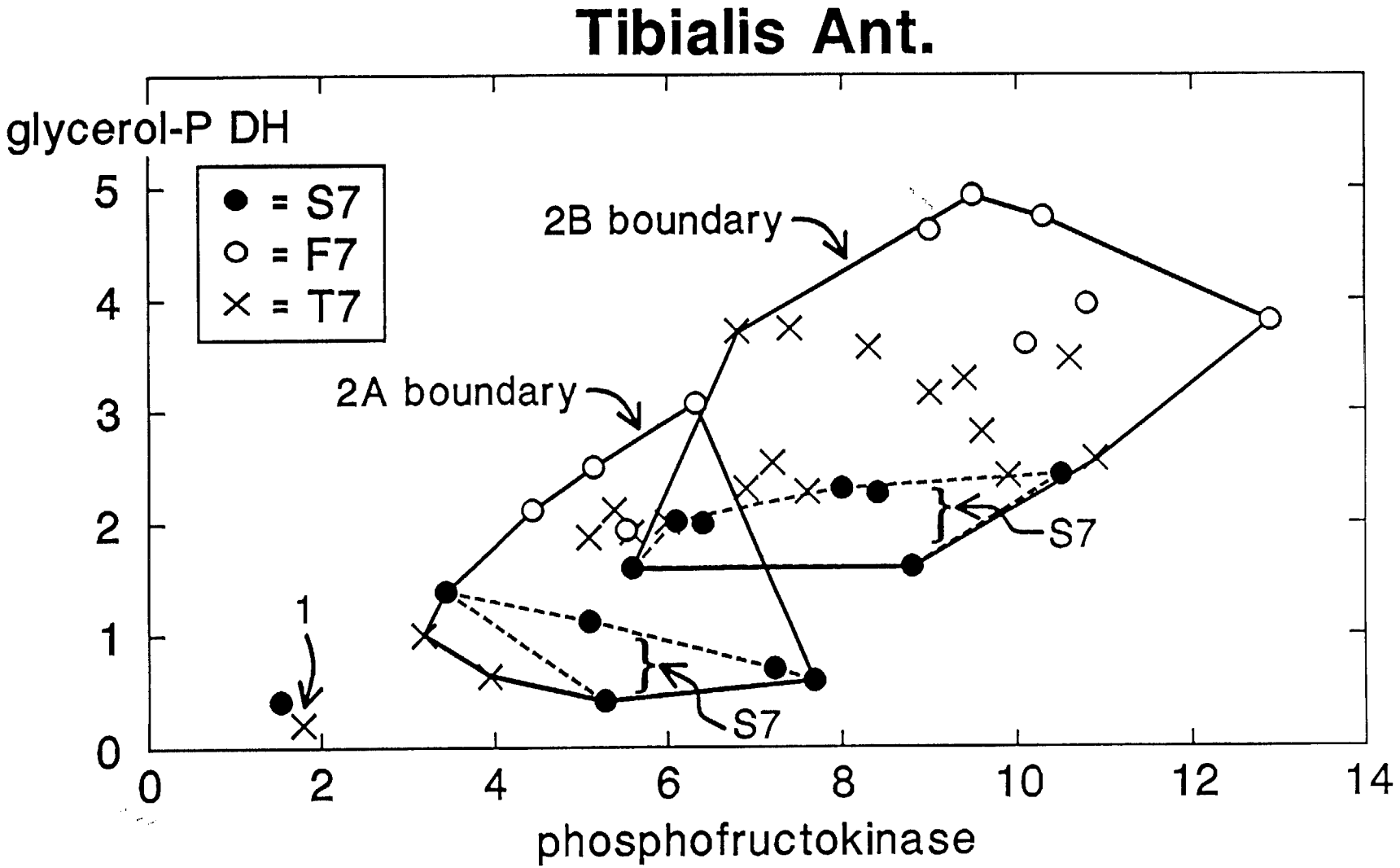
Tibialis Ant.
glycerol-P DH
● = S7
○ = F7
× = T7
2B boundary
2A boundary
S7
S7
1
0
1
2
3
4
5
0
2
4
6
8
10
12
14
phosphofructokinase

FIG. 16

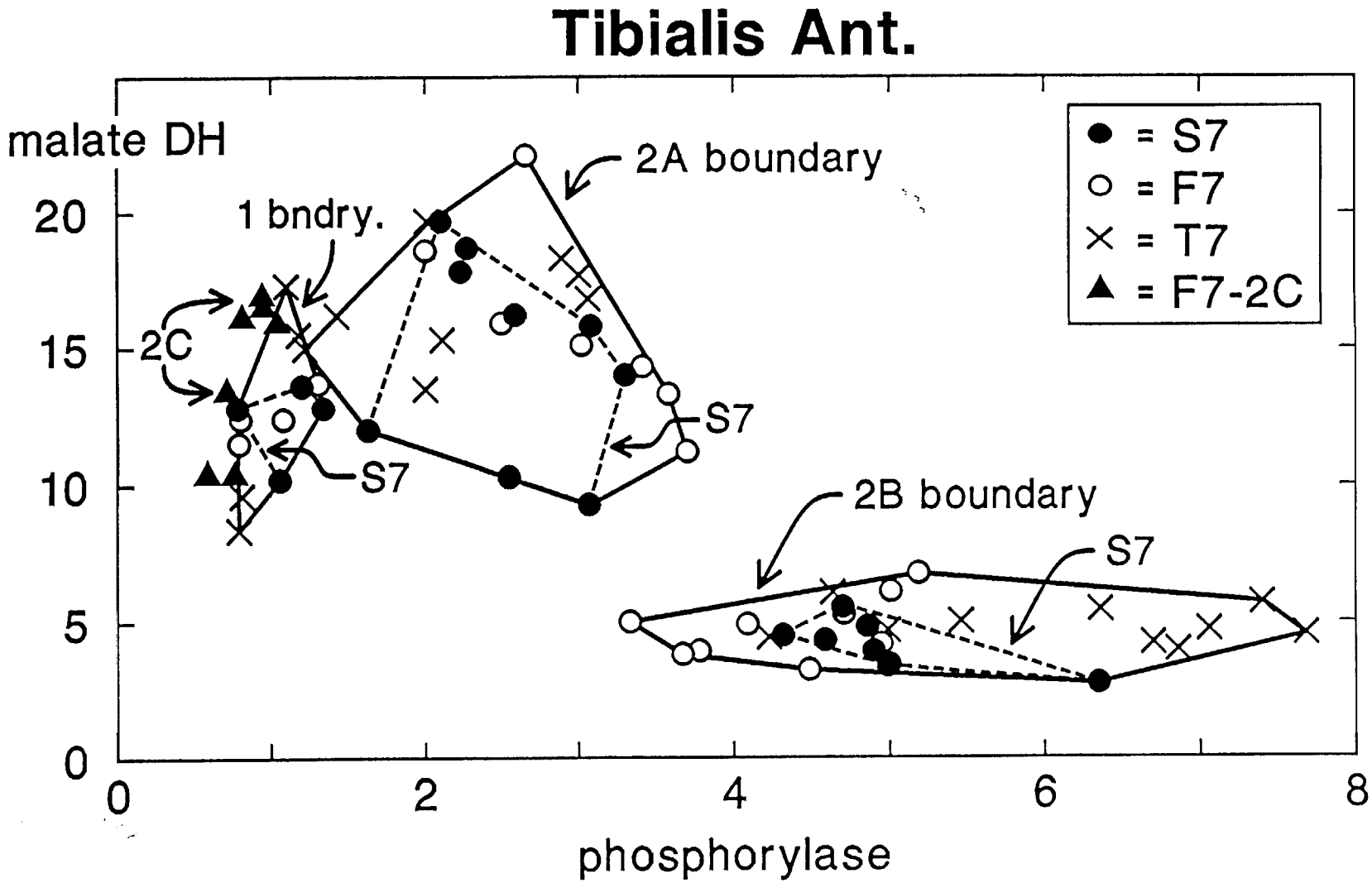
Tibialis Ant.
malate DH
20
15
10
5
0
0
2
4
6
8
phosphorylase
1 bndry.
2A boundary
2C
S7
S7
2B boundary
S7
● = S7
○ = F7
× = T7
▲ = F7-2C

Figure Legends - PART I

Figure 1. Glycerol-P dehydrogenase and pyruvate kinase levels in the same individual S6 and S7 soleus fibers. Activities are recorded as mol h^{-1} kg^{-1} (dry weight) at 20°C.

Figures 2 and 3. The same as Fig. 1 but for F6 + F7 and T6 + T7 fibers, respectively. The boundary for S6 + S7 fibers is shown in each case.

Figure 4. Hexokinase and pyruvate kinase levels in the same individual S6 and S7 soleus and S6 and S7 TA fibers. Activities are recorded as in Fig. 1.

Figures 5 and 6. The same as Fig. 4 but for F6 + F7 and T6 + T7 fibers, respectively. The boundary for S6 + S7 fibers is shown.

Figure 7. Fiber size (μg/mm) and MDH levels in the same individual soleus S6 and S7 fibers. MDH activity is recorded as for the enzymes of Fig. 1.

Figures 8 and 9. The same as Fig. 7 but for F6 + F7 and T6 + T7, respectively. The boundary for S6 and S7 fibers is shown.

Figure 10. Hexokinase and MDH levels in the same individual TA, S6 + S7 and F6 + F7 fibers. Activities are recorded as in Fig. 1.

Figure 11. The same as Fig. 10 but for S6 + S7 and T6 + T7.

Figure 12. Fiber size (μg/mm) and hexokinase levels in the same individual TA, S6 and S7 fibers. Hexokinase activity is recorded as for the enzymes of Fig. 1.

Figure 13. The same as Fig. 12 but for T6 and T7. The boundary for S6 + S7 is shown.

Figure 14. Thiolase (mitochondrial) levels in TA S6 and S7 individual fibers. Also shown are entries representing those individual fibers from the two flight and two tail suspension muscle that fall outside the domain of the S6 + S7 fibers. These outside fibers are designated F and f respectively for those from F6 and F7 muscles, and T and t for those from T6 and T7 muscles. Activities are recorded as for Fig. 1.

Figure 15. GOPDH and phosphofructokinase levels in individual TA fibers obtained from S7, F7 and T7 muscles and typed by myosin ATPase staining. Activities are recorded as in Fig. 1.

Figure 16. MDH and phosphorylase levels in individual TA fibers obtained from S7, F7, and T7 muscles and typed by myosin ATPase staining. Activities are recorded as in Fig. 1.

PART II. The distribution of selected enzymes and amino acids in the hippocampal formation.

Six key metabolic enzymes plus glutaminase and glutamate decarboxylase, as well as glutamate, aspartate and GABA, were measured in 11 regions of the hippocampal formation of synchronous, flight and tail suspension rats. Major differences were observed in the normal distribution patterns of each enzyme and amino acid, but no substantive effects of either microgravity or tail suspension on these patterns were clearly demonstrated.

All of the assays were performed with samples dissected from 20 μm freeze dried coronal microtome sections. The size of the samples and preparation for assay varied with the substance to be measured. In the case of aspartate and glutamate samples from the 11 hippocampal areas, weighing 30-50 ng, were heated in 0.5 μl of NaOH to destroy tissue enzymes and NAD^+; 0.1 μl of this was used for glutamate and 0.4 μl for aspartate. In addition a larger sample (1-1.5 μg) from three larger subdivisions of the hippocampus from additional rats were assayed for aspartate alone.

For GABA, samples weighing about 200 ng were heated in 0.1 μl of dilute HCl to destroy tissue enzymes and NADPH, and then incubated with 0.06 μl of the specific reagent. Samples for glutamate decarboxylase (GAD) were of about the same size. These were added directly to the specific reagent and incubated for 2 hours to increase the proportion of GABA formed from glutamate relative to preformed GABA which constituted a tissue blank.

The six metabolic enzymes were measured in each case in a single 150-300 ng sample which was dispersed in 5 μl of medium similar to that used for multiple enzyme assays of the muscle samples, and which likewise allowed indefinite storage without loss at -70°C. Duplicate 0.2 μl aliquots (0.1 μl for pyruvate kinase) were then used for each separate enzyme assay.

Glutaminase, which did not tolerate storage in this special medium, was measured in individual samples and added directly to the specific reagent. For separate assays of the 11 hippocampal areas, samples weighing 10-25 ng were added to 2 μl of reagent. For the assay of larger hippocampal subdivisions, samples weighing about 600 ng were added to 10 μl of reagent.

All of the methods employed were based on the conversion of NAD^+ to NADPH, NADH to NAD^+, or NADPH to $NADP^+$. The amount of pyridine product formed varied from about 1×10^{-12} mole in the aspartate assays to about 200×10^{-12} mol in the pyruvate kinase assays. It was therefore in all cases necessary to increase the sensitivity 1,000 to 10,000-fold by enzymatic cycling.

Six enzymes of energy metabolism.

Hexokinase (Fig. 17) was most active in CA1 with a peak in stratum radiatum and levels almost as high in the CA1 molecular layer. Lowest levels were found in CA3 with intermediate hexokinase levels in fascia dentata. The lowest consistent activities were in the pyramidal layer of CA3. The exceptionally high level in stratum oriens of T6 should be checked with brains from other tail suspension animals.

Pyruvate kinase (Fig. 18) located near the other end of the glycolytic pathway, was also highest in radiatum of CA1, but levels in the other parts of CA1 were not especially high and lowest average levels were found in fascia dentata.

Citrate synthase (Fig. 19), responsible for the first step in the citrate cycle, was like hexokinase highest among subdivisions of CA1 and lowest in CA3. The peak level was, however, in the molecular layer instead of radiatum of CA1 with the molecular layer of fascia dentata a close second.

β-hydroxyacyl CoA dehydrogenase (βOAC) (Fig. 20), the catalyst for a key step in fatty acid oxidation, was in contrast to the three previous enzymes, present at by far the highest levels among layers of fascia dentata, with CA1 a poor second. Note the extreme contrast between the relative positions of this enzyme and the positions of hexokinase and pyruvate kinase in radiatum of CA1. In spite of this general contrast, the highest levels for both βOAC and citrate synthase were found in the molecular layers.

Glucose-6-P dehydrogenase (G6PDH) (Fig. 21) and especially aspartate aminotransferase (Fig. 22) varied the least among the different regions. In the case of G6PDH, some attention should be given to the generally higher levels in many of the T6 regions.

In this regard, there are quite a few instances where enzyme activities of F8 or T6 deviate substantially from corresponding activities in S7. Note, however, that the range in most figures is only between 60% and 100%. Nevertheless, it may be possible and desirable to check on some of the largest deviations by analysis of samples from other S, F and T brains.

Glutaminase.

This enzyme, associated with the role of glutamate as a transmitter, showed a wider range of activities than any of the above six purely metabolic enzymes (Fig. 23). Moreover, the distribution did not resemble that of any of these. Note that levels were on average at least as high in CA3 as in CA1, and that the levels were relatively high in stratum oriens of both CA3 and CA1 and in hylus of fascia dentata, all regions which were in general on the low end of the scale for the metabolic enzymes. Because glutaminase levels in T6 were consistently low in CA1 and CA3, this enzyme was measured in three larger samples from each of S8, S10, F8, F9, T6 and T9. These samples encompassed all the layers analyzed in Figs. 17-23 from CA1, CA3 and fascia dentata respectively (Fig. 24). Although it seems quite obvious that there are some substantial differences among the several brains, there is no sign of consistent differences attributable to flight or tail suspension. Note that in all three of these gross regions, levels are higher for S8 than S10 and higher for F9 than F8.

Glutamate and Aspartate.

Both glutamate and aspartate varied over about a 30% range among the 12 subdivisions of the hippocampal formation analyzed (Fig. 25). There was a statistically significant correlation between aspartate and glutamate of S7 ($r=0.605$, $P < 0.05$) but not between these two amino acids for F8.

There was also a highly significant correlation between glutamate levels of S7 and F8 ($r=0.832$, $p < 0.01$) but not between aspartate levels of S7 and F8. Because of this and because aspartate appeared substantially higher in F8 than S7 for 3 portions of CA1, and lower in all but 1 portion of CA3, CA4, and fascia dentata (Fig. 9), aspartate concentrations were determined as in the case of glutaminase in 3 larger samples from each of S8, S10, F8, F9, T6, and T9. These samples were respectively comprised of all the segments represented in either the CA1, CA3 or fascia dentata zones of Fig. 25. The results (Fig. 26) show that aspartate is higher in S10 than S8 in each of the 3 zones, lower in F9 than F8 in each of the 3 zones, and higher in T9 than T6 in each of the 3 zones. Thus, consistent and substantial differences in aspartate concentrations do exist within the hippocampus of different rats. However, there is no significant difference on this score between synchronous and flight hippocampi or synchronous and tail suspension hippocampi.

Glutamate decarboxylase (GAD) and GABA (Tables 5 and 6)

GAD was consistently highest in the molecular layers of CA1 and fascia dentata and pyramidal layers of CA1. Lowest levels were observed in stratum oriens and radiatum (Figs. 27, 28). This enzyme was also subject to wide variation; note especially the differences in levels between S7 and S9 in four of the subdivisions of CA3 and fascia dentata. This makes it difficult to come to any conclusion about possible effects of flight or tail suspension.

GABA data were somewhat more consistent (Figs 29, 30). Relatively high levels were also found in the pyramidal cell and molecular layers, and the concentrations in the granular layer of fascia dentata were among the highest. There was no sign of consistent effects of flight or tail suspension on the GABA levels.

TABLE 5. GLUTAMATE DECARBOXYLASE DISTRIBUTION AMONG ELEVEN AREAS OF THE HIPPOCAMPAL FORMATION

AREA	S7	S9	F8	F10	T6	A11
CA1						
Oriens	14.5 (6) ± 1.8	17.8 (3) ± 0.9	18.4 (5) ± 2.8	16.5 (3) ± 2.5	21.3 (5) ± 1.8	17.7 ± 1.1
Pyramidalis	35.1 (6) ± 4.4	30.6 (4) ± 1.0	31.5 (4) ± 3.3	31.7 (3) ± 1.0	43.1 (6) ± 1.2	34.4 ± 2.3
Radiatum	21.3 (4) ± 1.0	17.4 (5) ± 0.8	21.7 (4) ± 1.4	20.7 (3) ± 1.0	18.5 (8) ± 0.8	19.9 ± 0.8
Molecularis	38.0 (7) ± 1.0	32.1 (3) ± 2.3	36.2 (6) ± 3.7	30.8 (3) ± 2.7	39.3 (7) ± 1.0	35.3 ± 1.6
CA3						
Oriens	25.1 (3) ± 2.4	21.0 (3) ± 3.1	34.4 (6) ± 4.1	17.5 (3) ± 0.5	27.5 (6) ± 4.4	25.1 ± 2.9
Pyramidalis	28.3 (2) ± 3.4	22.9 (3) ± 1.6	36.6 (5) ± 3.5	18.6 (3) ± 1.0	32.5 (5) ± 4.1	27.8 ± 3.2
Radiatum	33.4 (7) ± 2.1	16.9 (3) ± 0.3	19.4 (6) ± 1.6	16.4 (3) ± 0.6	24.8 (5) ± 0.9	22.2 ± 3.2
CA4						
Pyramidalis	23.6 (2) ± 0.8	21.0 (4) ± 1.3	27.1 (3) ± 1.0	27.2 (3) ± 1.6	21.0 (2) ± 3.8	24.0 ± 1.4
Fascia dentata						
Molecularis	45.6 (8) ± 3.8	24.6 (3) ± 1.2	38.5 (4) ± 4.9	46.1 (4) ± 2.9	49.9 (7) ± 2.4	40.9 ± 4.5
Granularis	21.7 (3) ± 0.5	36.1 (4) ± 1.4	22.1 (3) ± 0.5	40.8 (2) ± 2.0	--	30.2 ± 4.9
Hylus	28.0 (3) ± 2.0	22.1 (3) ± 2.0	24.6 (2) ± 3.0	26.4 (3) ± 2.2	23.5 (3) ± 0.5	24.9 ± 1.0

TABLE 6. GABA DISTRIBUTION AMONG ELEVEN AREAS OF THE HIPPOCAMPAL FORMATION

AREA	S7	S9	F8	F10	T6	A11
CA1						
Oriens	6.0 (7) ± 0.2	8.3 (4) ± 0.3	13.5 (4) ± 0.6	8.4 (4) ± 0.6	7.2 (6) ± 0.8	8.7 ± 1.3
Pyramidalis	12.3 (9) ± 0.9	11.9 (6) ± 0.4	15.6 (3) ± 2.5	15.2 (3) ± 1.7	10.3 (6) ± 0.4	13.0 ± 1.0
Radiatum	10.0 (4) ± 0.3	8.8 (6) ± 0.2	10.3 (3) ± 1.0	9.0 (4) ± 0.2	10.1 (3) ± 0.4	9.6 ± 0.3
Molecularis	13.0 (7) ± 0.6	13.3 (5) ± 1.0	16.0 (5) ± 0.5	13.0 (4) ± 0.3	13.3 (5) ± 0.6	13.7 ± 0.5
CA3						
Oriens	8.3 (3) ± 1.9	14.7 (6) ± 1.5	11.8 (5) ± 1.1	15.0 (3) ± 0.3	10.5 (6) ± 0.9	12.4 ± 1.2
Pyramidalis	15.0 (5) ± 0.6	19.2 (5) ± 1.4	16.5 (4) ± 0.9	18.4 (2) ± 0.1	15.6 (5) ± 0.8	16.9 ± 0.8
Radiatum	14.7 (7) ± 0.4	15.0 (6) ± 0.5	12.0 (5) ± 1.0	12.2 (3) ± 0.6	14.7 (5) ± 0.4	13.8 ± 0.5
CA4						
Pyramidalis	14.8 (7) ± 0.8	15.1 (5) ± 1.1	13.9 (2) ± 0.1	14.8 (4) ± 0.6	16.8 (2) ± 0.1	15.0 ± 0.4
Fascia dentata						
Molecularis	15.8 (7) ± 0.5	16.3 (5) ± 1.4	18.7 (6) ± 1.7	14.1 (3) ± 0.4	16.3 (3) ± 0.2	16.2 ± 0.7
Granularis	15.8 (4) ± 0.3	20.9 (4) ± 0.9	14.9 (4) ± 0.6	18.1 (4) ± 2.1	15.0 (4) ± 0.5	17.2 ± 1.1
Hylus	14.7 (3) ± 1.5	13.6 (8) ± 1.0	13.2 (3) ± 0.8	11.7 (3) ± 0.8	15.6 (2) ± 0.2	13.8 ± 0.6

Fig 17

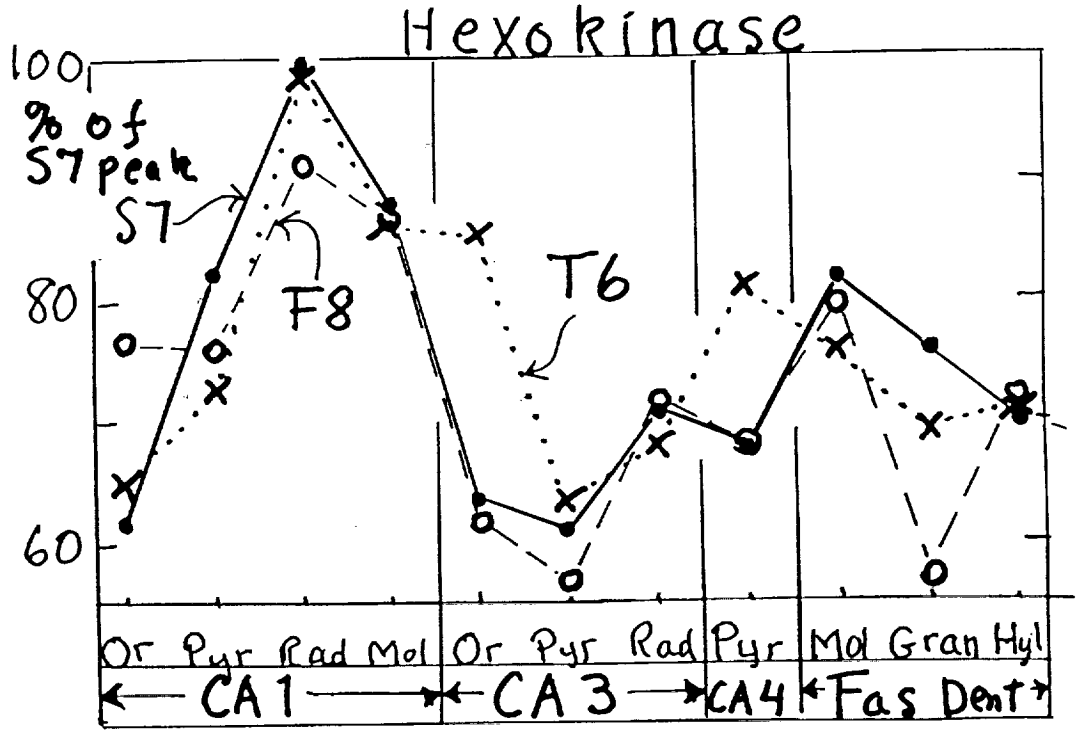
Hexokinase
100
% of
S7 peak
80
60
S7
F8
T6
Or Pyr Rad Mol Or Pyr Rad Pyr Mol Gran Hyl
CA1
CA3
CA4
Fas Dent

Fig 18

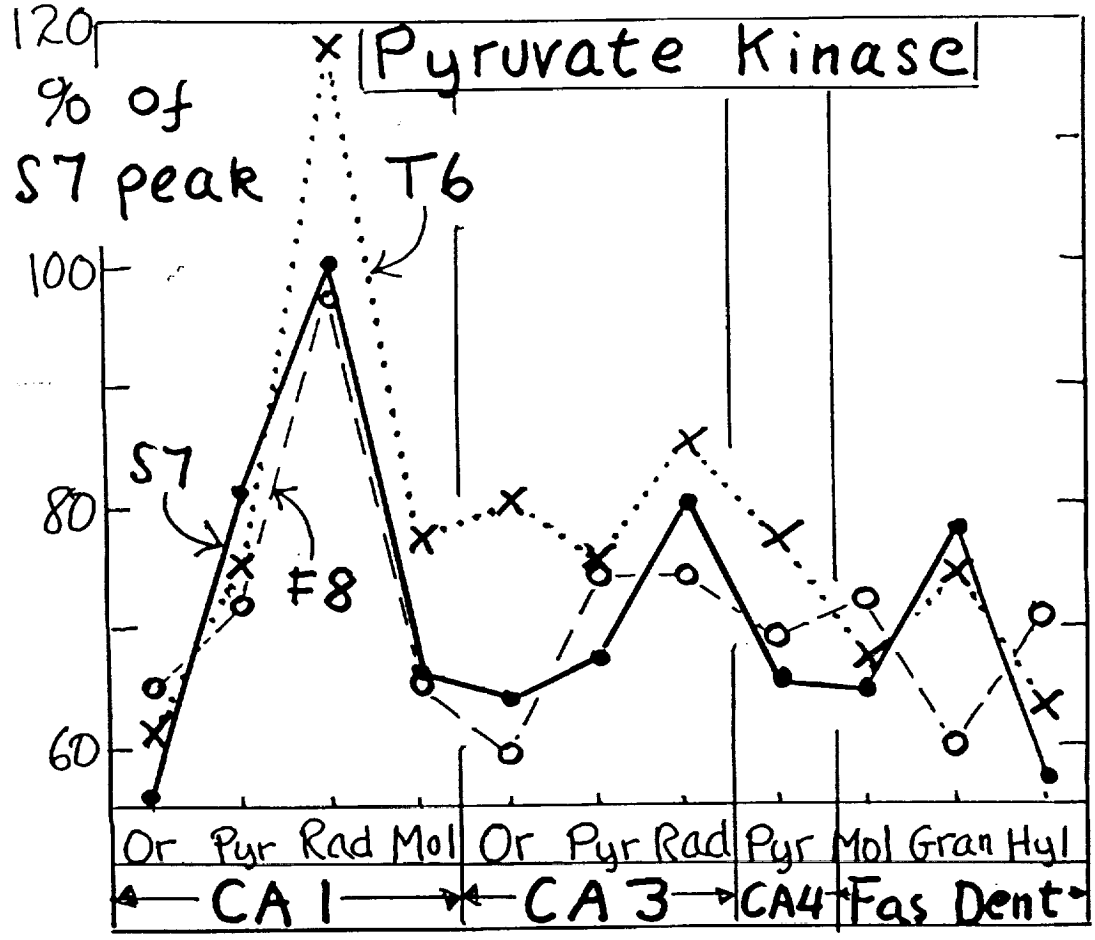
Pyruvate Kinase
120
% of
S7 peak
100
80
60
T6
S7
F8
Or
Pyr
Rad
Mol
Or
Pyr
Rad
Pyr
Mol
Gran
Hyl
CA 1
CA 3
CA4
Fas Dent

Fig 19

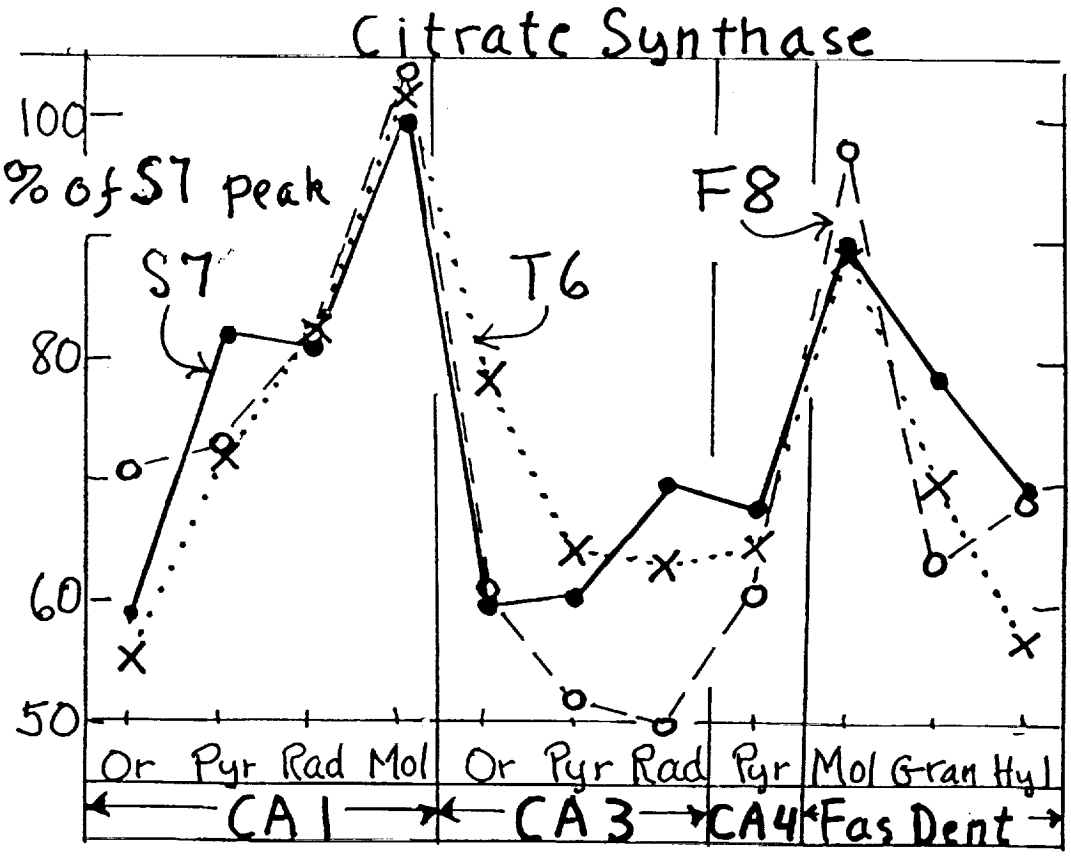
Citrate Synthase
100
% of S7 peak
80
60
50
S7
T6
F8
Or Pyr Rad Mol Or Pyr Rad Pyr Mol Gran Hyl
CA1
CA3
CA4
Fas Dent

Fig 20

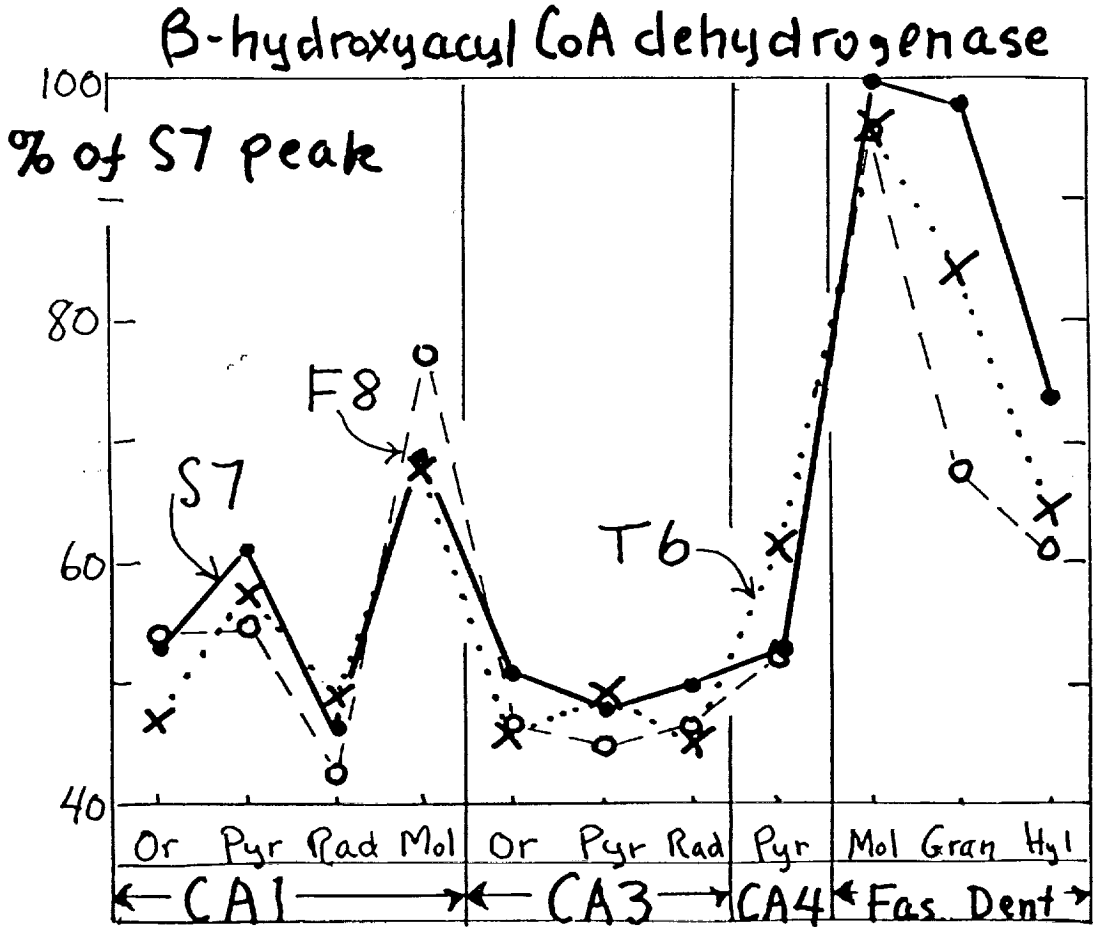
β-hydroxyacyl CoA dehydrogenase
100
% of S7 peak
80
60
40
S7
F8
T6
Or
Pyr
Rad
Mol
Or
Pyr
Rad
Pyr
Mol
Gran
Hyl
CA1
CA3
CA4
Fas. Dent

Fig 21

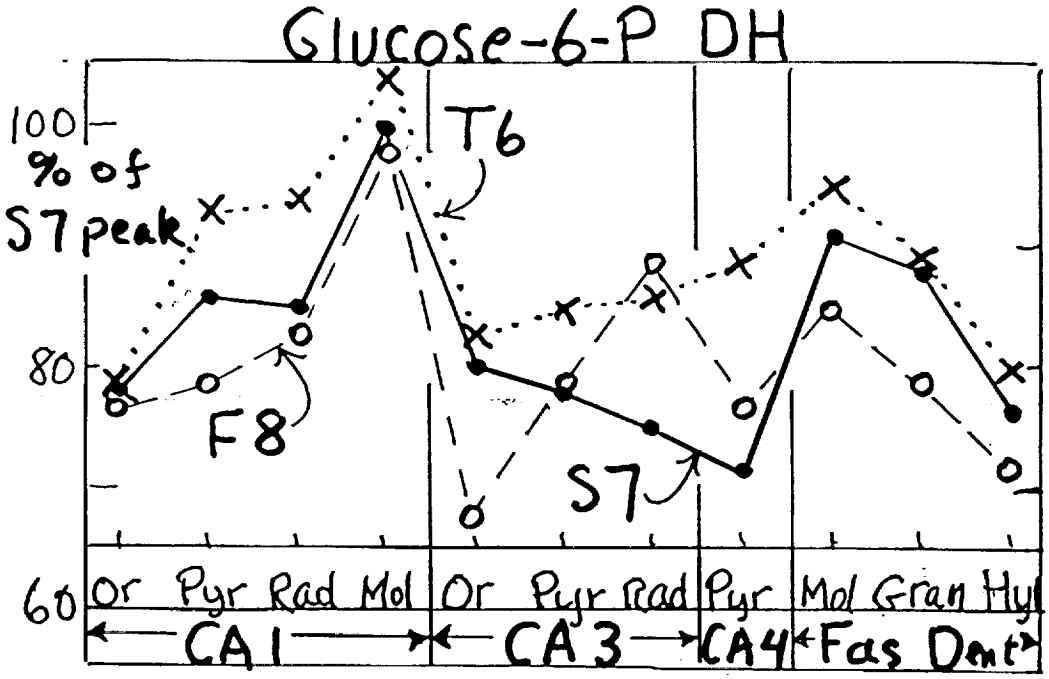
Glucose-6-P DH
100
% of
S7 peak
80
60
T6
F8
S7
Or Pyr Rad Mol
Or Pyr Rad
Pyr
Mol Gran Hyl
CA1
CA3
CA4
Fas Dnt

Fig22

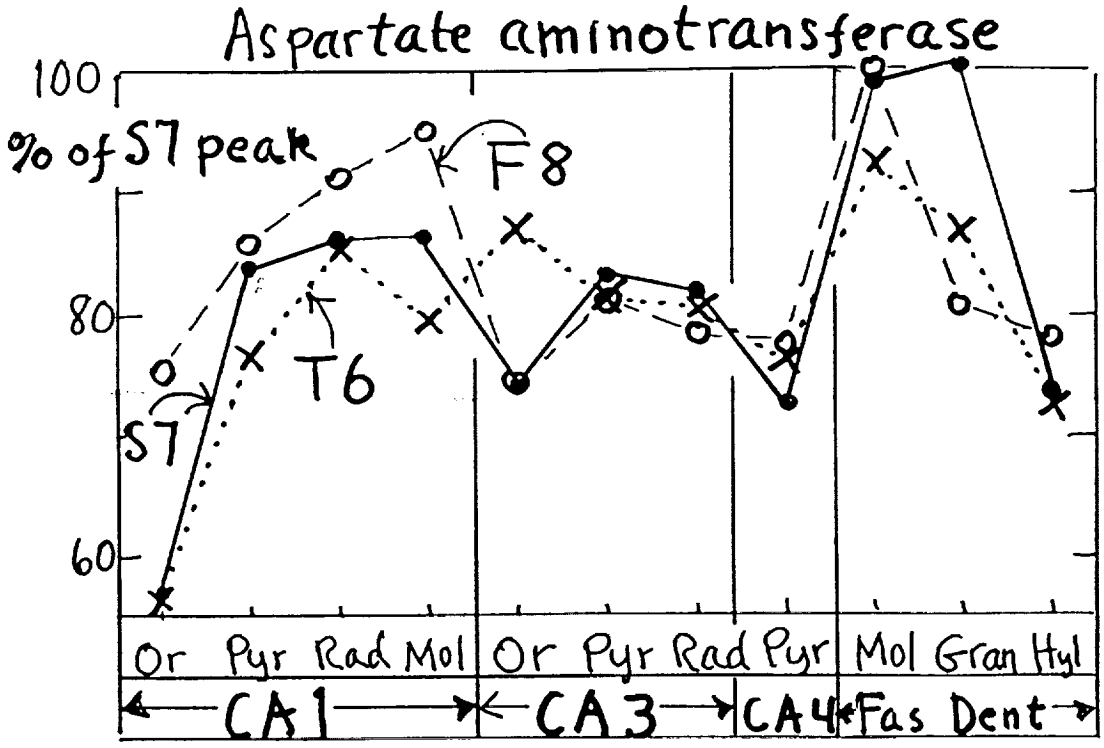
Aspartate aminotransferase
100
% of S7 peak
80
60
S7
T6
F8
Or Pyr Rad Mol Or Pyr Rad Pyr Mol Gran Hyl
CA1
CA3
CA4
Fas Dent

Fig 23

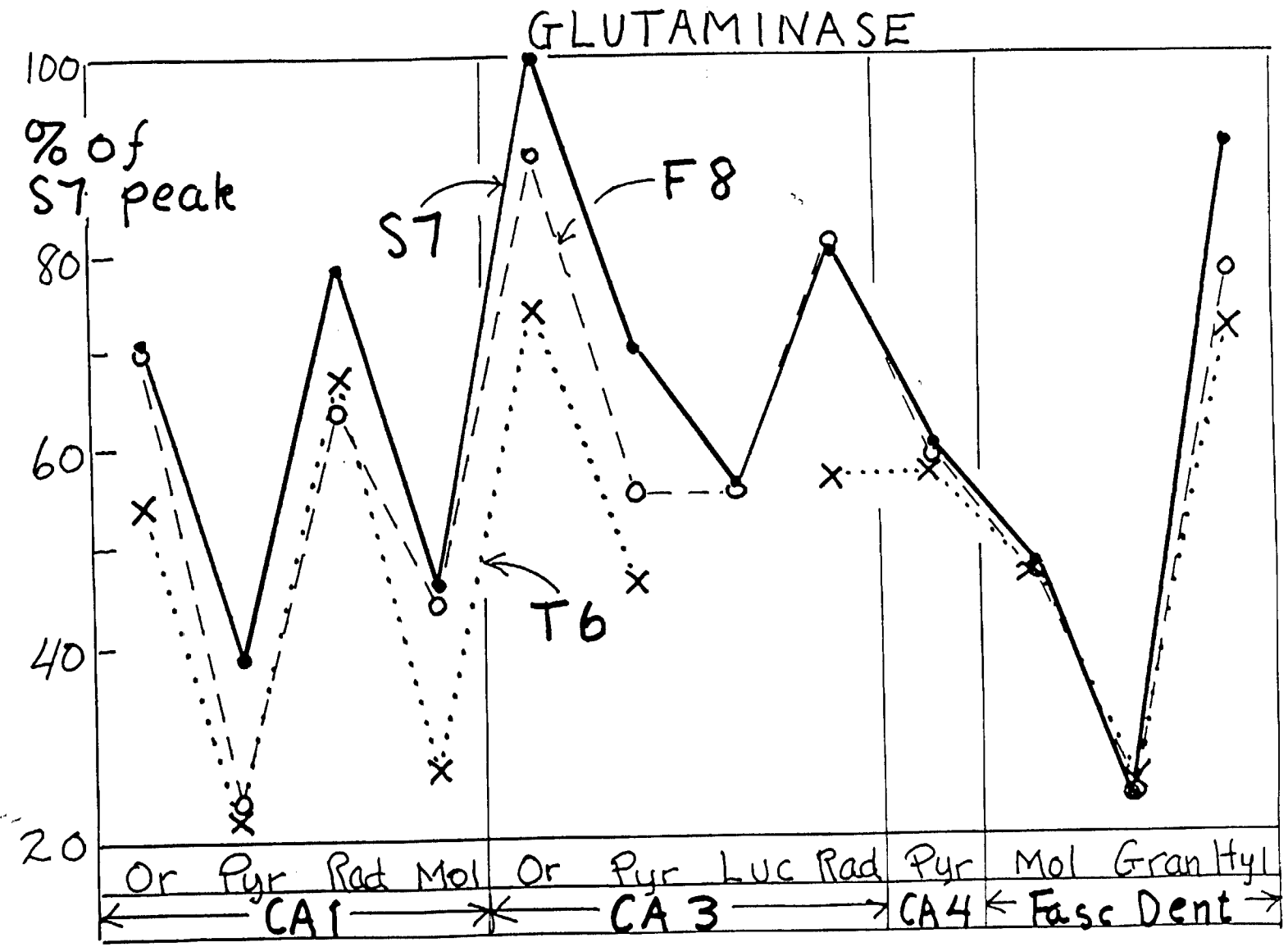
GLUTAMINASE
100
% of
S7 peak
80
60
40
20
S7
F8
T6
Or
Pyr
Rad
Mol
Or
Pyr
Luc
Rad
Pyr
Mol
Gran
Hyl
CA1
CA3
CA4
Fasc Dent

Fig 24

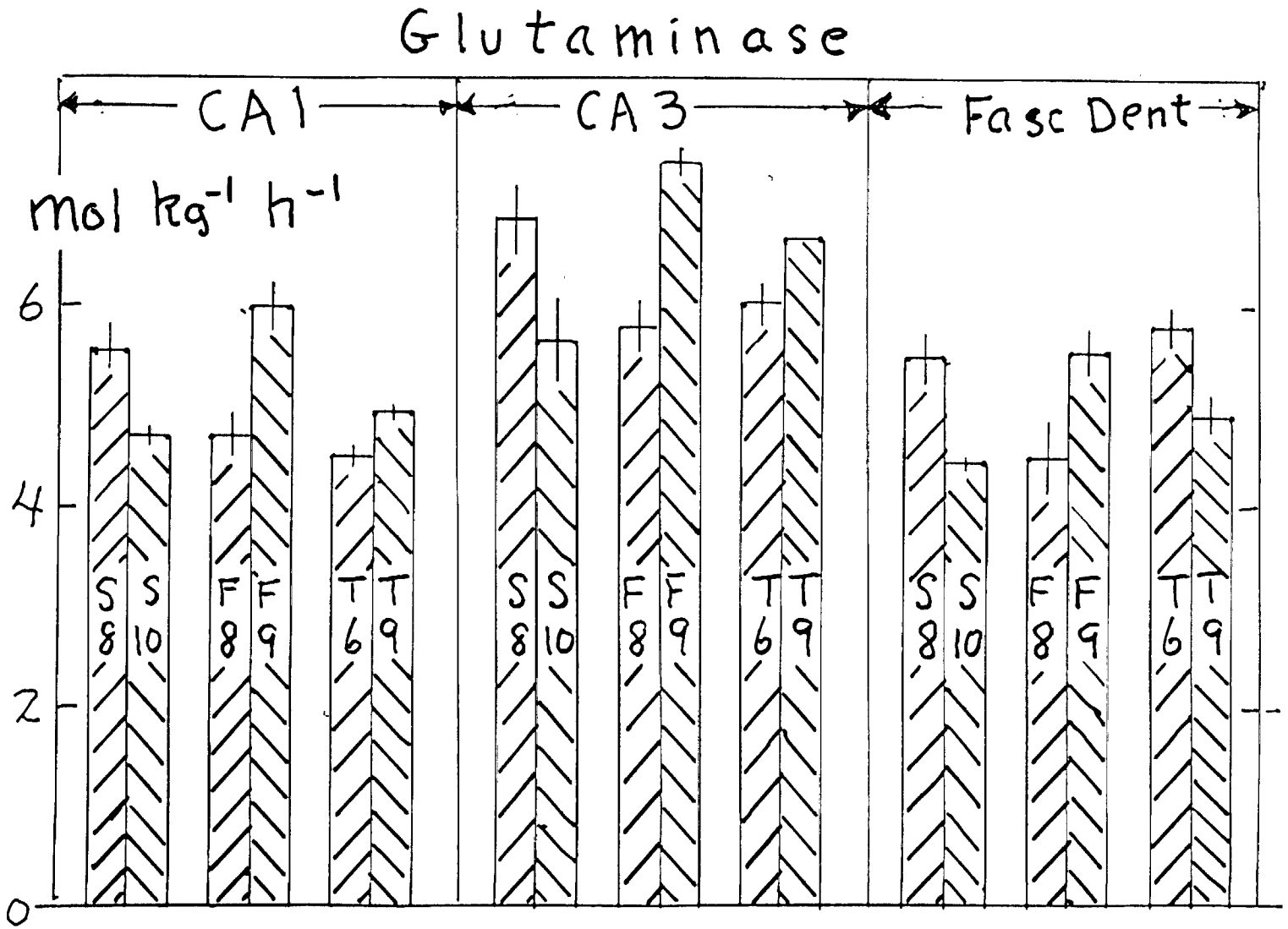
Glutaminase
CA1
CA3
Fasc Dent
mol kg-1 h-1
6
4
2
0
S 8
S 10
F 8
F 9
T 6
T 9

Fig 25

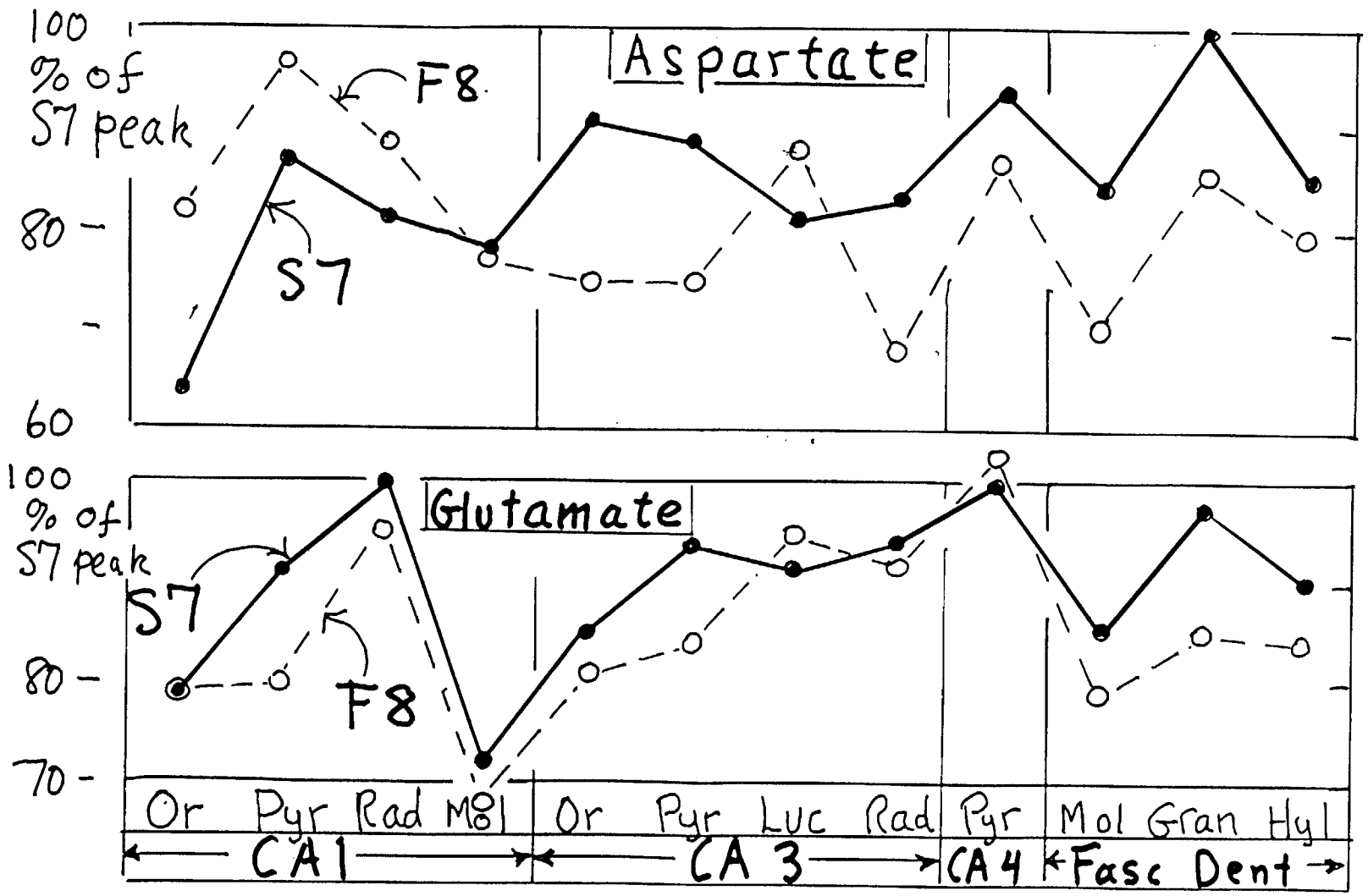
100
% of
S7 peak
80
60
F8
S7
Aspartate
100
% of
S7 peak
80
70
S7
F8
Glutamate
Or
Pyr
Rad
Mol
Or
Pyr
Luc
Rad
Pyr
Mol
Gran
Hyl
CA1
CA 3
CA 4
Fasc Dent

Fig 26

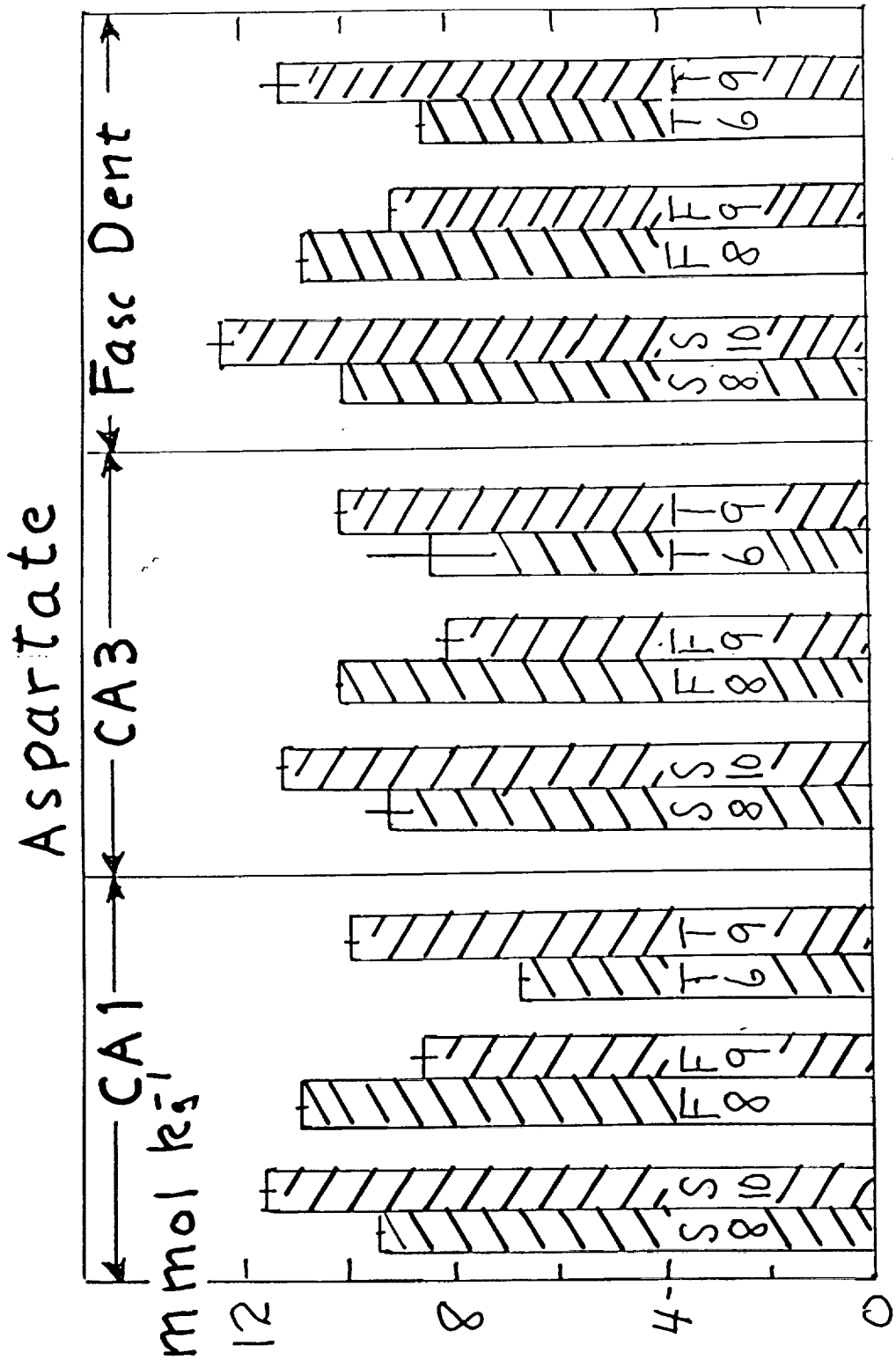

Fig 27

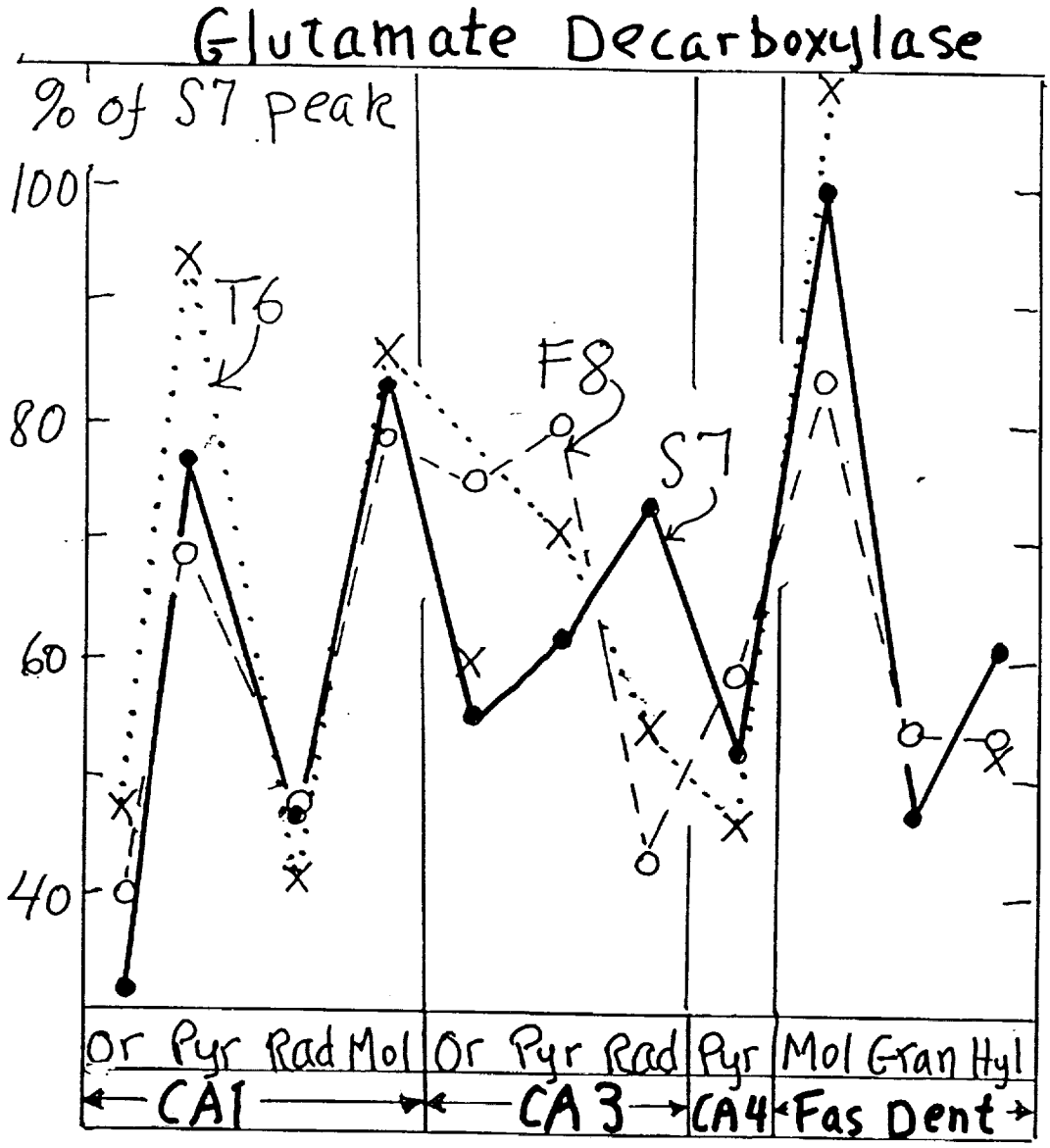
Glutamate Decarboxylase
% of S7 peak
100
80
60
40
T6
F8
S7
Or Pyr Rad Mol
Or Pyr Rad
Pyr
Mol Gran Hyl
CA1
CA3
CA4
Fas Dent

Fig 28

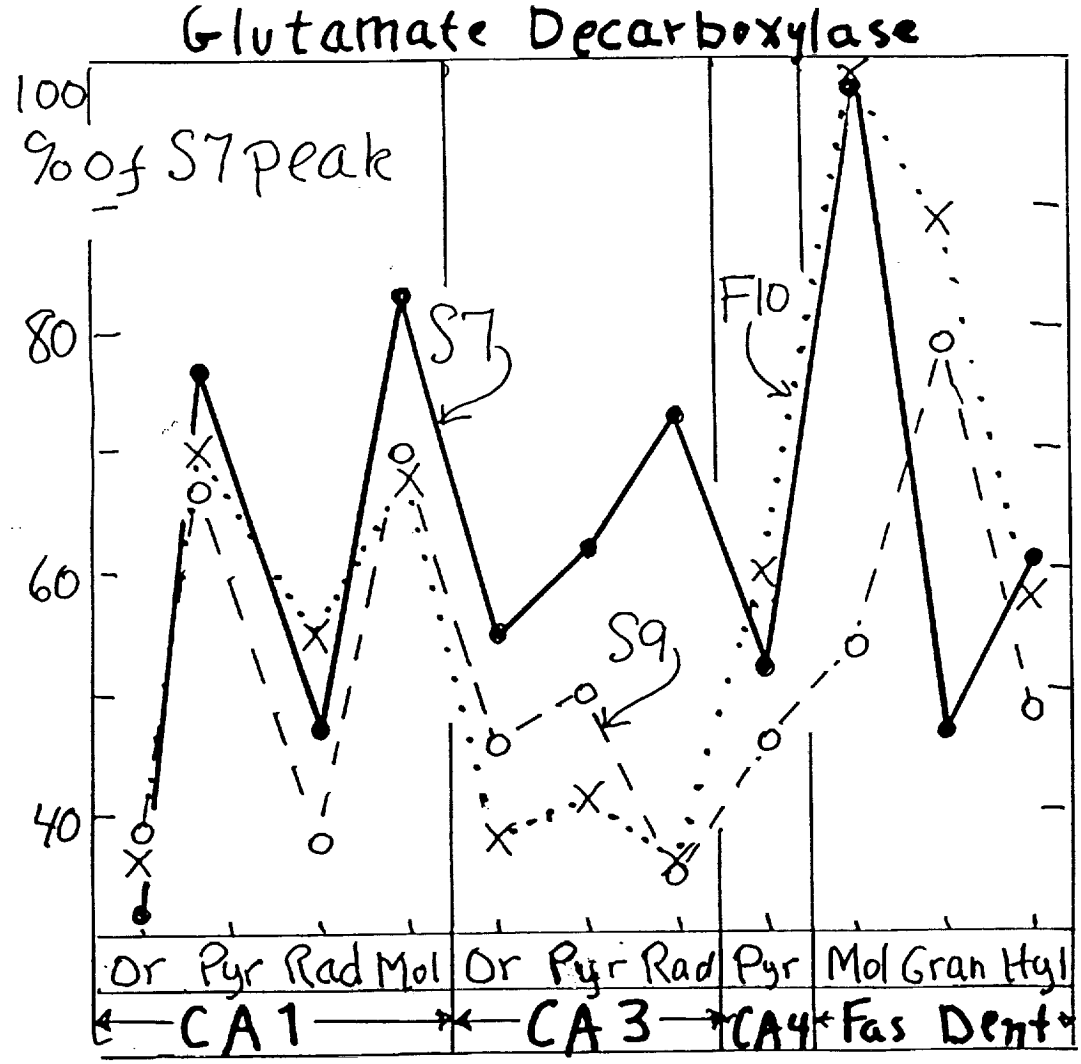
Glutamate Decarboxylase
100
% of S7 peak
80
60
40
S7
S9
F10
Or Pyr Rad Mol Or Pyr Rad Pyr Mol Gran Hyl
CA1
CA3
CA4
Fas Dent

Fig 29

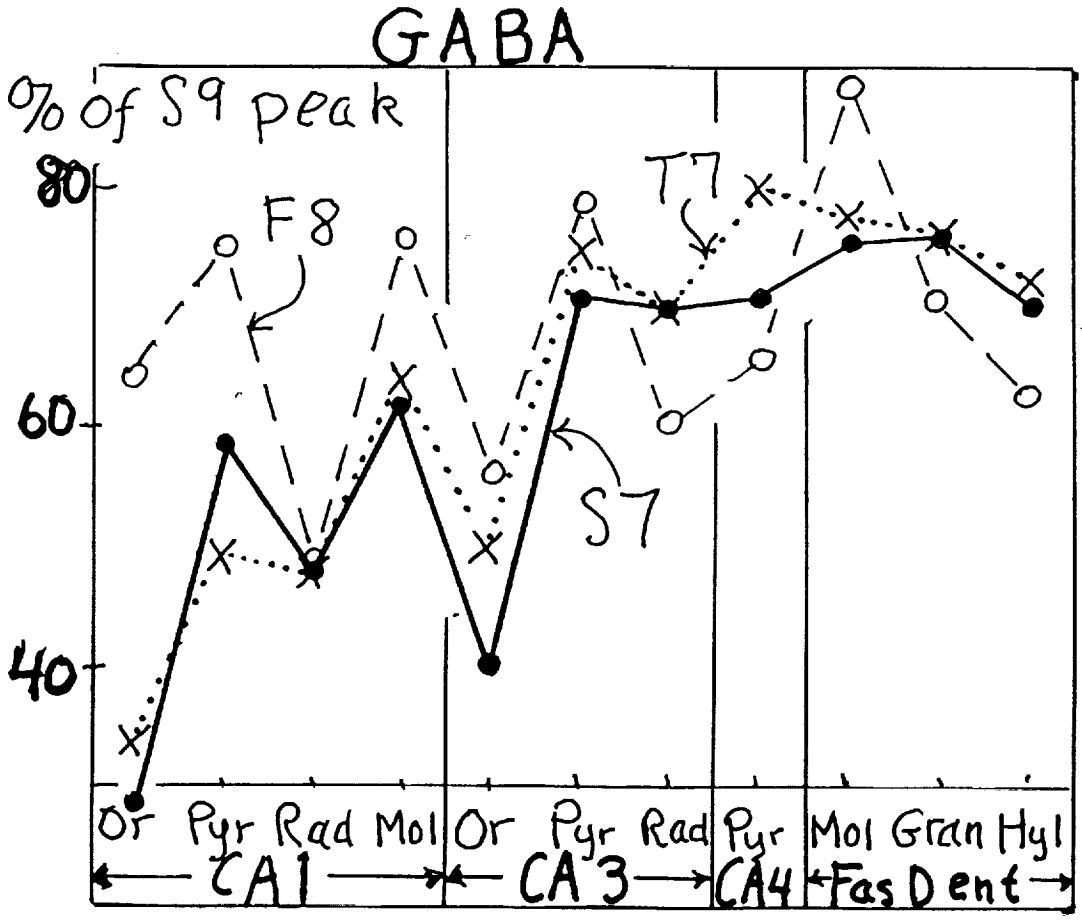
GABA
% of S9 peak
80
60
40
F8
T7
S7
Or Pyr Rad Mol Or Pyr Rad Pyr Mol Gran Hyl
CA1
CA3
CA4
Fas Dent

Fig 30

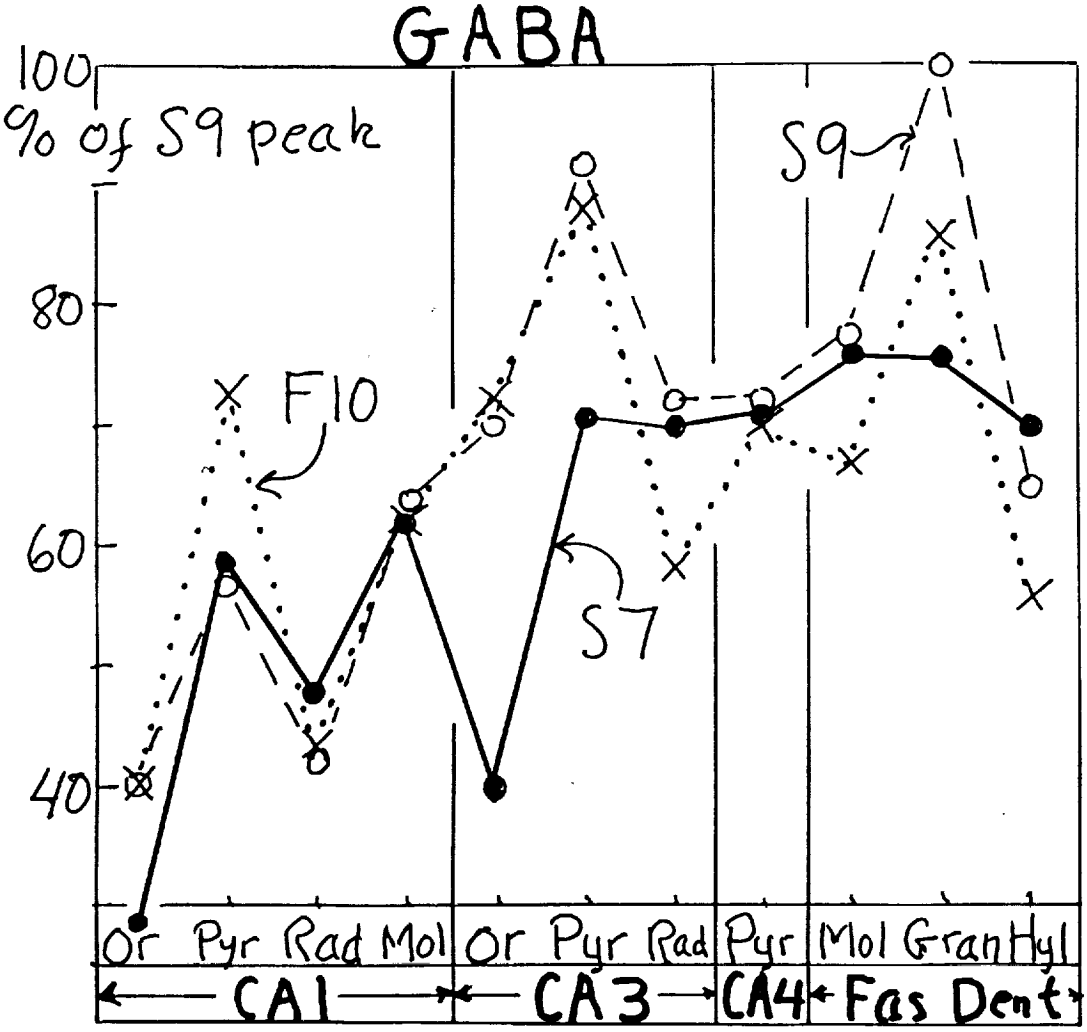
GABA
100
% of S9 peak
80
60
40
S9
F10
S7
Or Pyr Rad Mol
Or Pyr Rad
Pyr
Mol Gran Hyl
CA1
CA3
CA4
Fas Dent

Figure Legends - PART II

Figure 17. Hexokinase in hippocampal subdivisions of S7, F8 and T6. The peak activity in S7 was 8 mol kg^{-1} (dry) h^{-1} at 20°C. Abbreviations are: Or, Oriens; Pyr, pyramidalis; Rad, radiatum; Mol, molecularis; Gran, granularis; and Hyl, hylus.

Figure 18. Pyruvate kinase in hippocampal subdivisions of S7, F8 and T6. The peak level in S7 was 74 mol kg^{-1} (dry) h^{-1} at 20°C. Abbreviations as for Fig. 17.

Figure 19. Citrate synthase in hippocampal subdivisions of S7, F8 and T6. The peak activity in S7 was 11 mol kg^{-1} (dry) h^{-1} at 20°C. Abbreviations as for Fig. 17.

Figure 20. β-hydroxyacyl CoA dehydrogenase in hippocampal subdivisions of S7, F8 and T6. The peak activity in S7 was 1.7 mol kg^{-1} (dry) h^{-1} at 20°C. Abbreviations as for Fig. 17.

Figure 21. Glucose-6-phosphate dehydrogenase in hippocampal subdivisions of S7, F8 and T6. The peak activity in S7 was 0.36 mol kg^{-1} (dry) h^{-1} at 20°C. Abbreviations as for Fig. 17.

Figure 22. Aspartate aminotransferase in hippocampal subdivisions of S7, F8 and T6. The peak activity in S7 was 31 mol kg^{-1} (dry) h^{-1} at 20°C. Abbreviations as for Fig. 17.

Figure 23. Glutaminase levels in hippocampal subdivisions of S7, F8 and T6. The peak level in S7 was 8.6 mol kg^{-1} (dry) h^{-1} at 20°C. Abbreviations as for Fig. 17, plus Lu, stratum lucidum.

Figure 24. Bar graph of glutaminase levels in 3 major zones of hippocampus of S8, S10, F8, F9, T6 and T9. Standard errors are indicated.

Figure 25. Aspartate and glutamate in hippocampal subdivisions of S7 and S8. The peak levels in S7 were 14.6 and 73 mmol kg^{-1} (dry), respectively.

Figure 26. Bar graph of aspartate levels in 3 major hippocampal zones of S8, S10, F8, F9, T6 and T9.

Figures 27 and 28. GAD levels in hippocampal subdivisions of S7, S9, F8, F10 and T6. The peak activity in S7 was 46 mmol kg^{-1} (dry) h^{-1} at 38°C.

Figures 29 and 30. GABA levels in hippocampal subdivisions of S7, S9, F8, F10 and T6. The peak concentration in S9 was 21 mmol kg^{-1} (dry).